

MODELLING OF CHOLANGIOCARCINOGENESIS BY USING PLURIPOTENT STEM CELL



A Thesis Submitted in Partial Fulfillment of the Requirements  
for the Degree of Master of Science in Medical Sciences

Common Course

FACULTY OF MEDICINE

Chulalongkorn University

Academic Year 2020

Copyright of Chulalongkorn University

การสร้างแบบจำลองของการเกิดโรคมะเร็งท่อน้ำดี โดยการใช้เซลล์ต้นกำเนิดชนิดพหุศักยภาพ



วิทยานิพนธ์นี้เป็นส่วนหนึ่งของการศึกษาตามหลักสูตรปริญญาวิทยาศาสตรมหาบัณฑิต

สาขาวิชาวิทยาศาสตร์การแพทย์ ไม่สังกัดภาควิชา/เทียบเท่า

คณะแพทยศาสตร์ จุฬาลงกรณ์มหาวิทยาลัย

ปีการศึกษา 2563

ลิขสิทธิ์ของจุฬาลงกรณ์มหาวิทยาลัย

Thesis Title                                      MODELLING OF CHOLANGIOCARCINOGENESIS BY USING  
  PLURIPOTENT STEM CELL  
By    Miss Natthida Kittimawikrom  
Field of Study                                    Medical Sciences  
Thesis Advisor                                 Associate Professor NIPAN ISRASENA, M.D., Ph.D.

---

Accepted by the FACULTY OF MEDICINE, Chulalongkorn University in Partial  
Fulfillment of the Requirement for the Master of Science

..... Dean of the FACULTY OF MEDICINE  
(Professor SUTTIPONG WACHARASINDHU, M.D.)

THESIS COMMITTEE

..... Chairman  
(Assistant Professor AMORNPUN SEREEMASPUN, M.D.,  
Ph.D.)

..... Thesis Advisor  
(Associate Professor NIPAN ISRASENA, M.D., Ph.D.)

..... Examiner  
(SUPANSA YODMUANG, Ph.D.)

..... Examiner  
(Associate Professor WILAI ANOMASIRI, Ph.D.)

..... External Examiner  
(Associate Professor Pakpoom Kheolamai, M.D., Ph.D.)

ณัฐธิดา กิตติมาภิกรม : การสร้างแบบจำลองของการเกิดโรคมะเร็งท่อน้ำดี โดยใช้เซลล์ต้นกำเนิด  
 ชนิดพหุศักยภาพ . ( MODELLING OF CHOLANGIOCARCINOGENESIS BY USING  
 PLURIPOTENT STEM CELL) อ.ที่ปรึกษาหลัก : รศ. ดร. นพ.นิพัฏฐณ์ อิศรเสนา ณ อยุธยา

จากการศึกษาการหลั่งดับเอ็กโซมในโรคมะเร็งท่อน้ำดี การกลายพันธุ์ของยีน SMAD4 พบได้บ่อยใน  
 กลุ่มของผู้ป่วยมะเร็งท่อน้ำดี ซึ่งการกลายพันธุ์ของยีนนี้ส่งผลอย่างไรต่อการก่อให้เกิดโรคมะเร็งท่อน้ำดียังไม่เป็น  
 ที่ทราบแน่ชัด รวมถึงการศึกษาต้นกำเนิดของเซลล์มะเร็งท่อน้ำดียังไม่แน่ชัดว่าเกิดขึ้นจากเซลล์ใดภายในตับ  
 อยากรู้ดี ความเหมาะสมของแบบจำลองการศึกษาโรคมะเร็งท่อน้ำดีในปัจจุบัน ยังมีข้อจำกัดในแง่ของการใช้  
 เป็นตัวแทนเซลล์มนุษย์ รวมถึงข้อจำกัดในการติดตามกลไกการเปลี่ยนแปลงที่เกิดขึ้นในระยะเริ่มแรก งานวิจัยนี้มี  
 วัตถุประสงค์เพื่อศึกษาบทบาทของการกลายพันธุ์ของ *SMAD4* ในเซลล์ cholangiocyte progenitors เพื่อตอบ  
 คำถามดังกล่าว ผู้วิจัยได้นำเซลล์ต้นกำเนิดชนิดพหุศักยภาพ (induced pluripotent stem cells, iPSCs) มาทำ  
 การสร้าง cholangiocyte organoids ด้วยการเหนี่ยวนำโดย growth factors จากผลการศึกษาพบว่า เซลล์  
 cholangiocyte organoids ที่สร้างได้มีคุณสมบัติของ cholangiocyte progenitor ในการเพาะเลี้ยงได้ในระยะ  
 ยาว (>8 เดือน) และมีการแสดงออกของยีนที่เกี่ยวข้องกับเซลล์ท่อน้ำดี รวมถึงความสามารถของเซลล์ในการ  
 เปลี่ยนไปเป็นเซลล์ตับ ซึ่งชี้ให้เห็นว่าเซลล์ดังกล่าวสามารถนำมาใช้เป็นแบบจำลองของเซลล์ในการศึกษาโรคมะเร็ง  
 ท่อน้ำดีได้ นอกจากนี้ยังทำการสร้าง inducible *SMAD4* knockout iPSCs เพื่อศึกษาบทบาทการกลายพันธุ์ของ  
 ยีน *SMAD4* ด้วยเทคนิค CRISPR/Cas9 ใน cholangiocyte organoids จากผลการศึกษาการกลายพันธุ์ของยีน  
*SMAD4* ใน cholangiocyte organoid ผู้วิจัยพบว่า การกลายพันธุ์ของ *SMAD4* มีผลต่อความสามารถในการ  
 เพิ่มจำนวน และลดการตอบสนองต่อความเสียหายของดีเอ็นเอจากการฉายรังสีอย่างมีนัยสำคัญ รวมไปถึง  
 ความสามารถในการสร้างท่อของ cholangiocyte organoids โดยความรู้ที่ได้จากแบบจำลองการกลายพันธุ์ของ  
*SMAD4* ใน cholangiocyte organoids จะช่วยเพิ่มความเข้าใจในกลไกระยะเริ่มแรกของการเกิดโรคมะเร็งท่อน้ำดี  
 และเป็นประโยชน์ต่อการพัฒนาโมเดลโรคมะเร็งท่อน้ำดีในอนาคต

จุฬาลงกรณ์มหาวิทยาลัย  
 CHULALONGKORN UNIVERSITY

สาขาวิชา      วิทยาศาสตร์การแพทย์  
 ปีการศึกษา    2563

ลายมือชื่อนิสิต .....

ลายมือชื่อ อ.ที่ปรึกษาหลัก .....

# # 5974061730 : MAJOR MEDICAL SCIENCES

KEYWORD: SMAD4, CRISPR/Cas9, CCA

Natthida Kittimawikrom : MODELLING OF CHOLANGIOCARCINOGENESIS BY USING PLURIPOTENT STEM CELL. Advisor: Assoc. Prof. NIPAN ISRASENA, M.D., Ph.D.

The exome sequencing study of cholangiocarcinoma (CCA) revealed *SMAD4* mutation was frequently observed. The role of *SMAD4* to cholangiocarcinogenesis as well as cell origin of CCA are not fully understand. According to current CCA model including cell lines and animal models, it still limited in resembling human cells and early event during carcinogenesis. The objective of this study was to study the role of *SMAD4* signaling disruption in cholangiocyte progenitors. To clarify these questions, we used induced pluripotent stem cells (iPSCs) to differentiate into cholangiocyte organoids by using growth factors induction in this study. The result demonstrated that cholangiocyte organoids were revealed cholangiocyte progenitor potential to long-term propagate (>8 months) and cholangiocyte-associated genes including hepatocyte-like cell conversion capacity. Our findings indicated that cholangiocyte organoids could represent as modelling for further CCA study. Additionally, we generated inducible *SMAD4* knockout iPSC for *SMAD4* knockout study in cholangiocyte organoids by using CRISPR/Cas9. Loss of *SMAD4* in cholangiocyte organoids significantly affected on proliferation capacity, DNA damage-induced radiation response as well as tubular morphogenesis of cholangiocyte progenitors. The knowledge of *SMAD4* knockout in cholangiocyte progenitors will provide more understanding of early event mechanism during cholangiocarcinogenesis and beneficial to develop CCA model in further study.

จุฬาลงกรณ์มหาวิทยาลัย  
CHULALONGKORN UNIVERSITY

Field of Study: Medical Sciences

Student's Signature .....

Academic Year: 2020

Advisor's Signature .....

## ACKNOWLEDGEMENTS

First of all, I gratefully thank to my advisor Assoc. Prof. Nipan Israsena for giving me the opportunity to do this research. I am greatly appreciated for his suggestions. I would also like to thank my thesis committee: Asst. Prof. Amornpun Sereemasun, Dr. Supansa Yodmuang, Assoc. Prof. Wilai Anomasari and Assoc. and Prof. Pakpoom Kheolamai for comments and suggestions.

I would like to thank the members in Stem cell and Cell therapy research unit especially Dr. Praewphan Ingrungruanglert for her helps, comments, and suggestions. I would also like to thank to my lab buddy, Kamonchanok Kongsri, for her friendships and helps.

Finally, I would like to acknowledge with gratitude to my family. This achievement would not have been possible without them.

Natthida Kittimawikrom

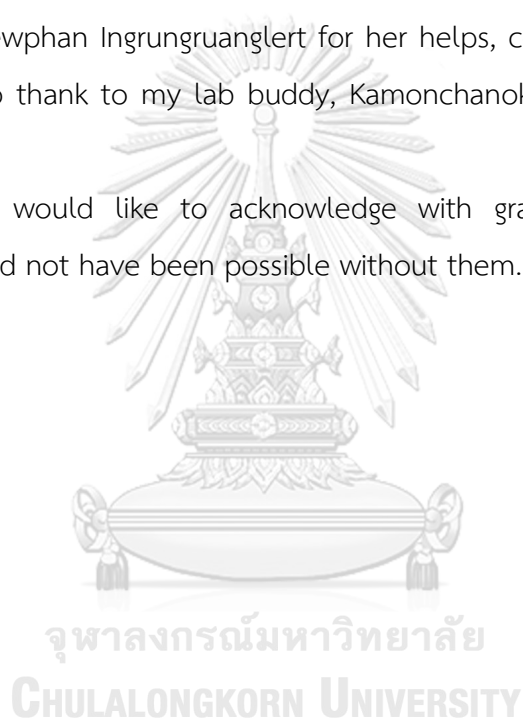


## TABLE OF CONTENTS

	Page
ABSTRACT (THAI) .....	iii
ABSTRACT (ENGLISH) .....	iv
ACKNOWLEDGEMENTS.....	v
TABLE OF CONTENTS.....	vi
LIST OF TABLES .....	ix
LIST OF FIGURES .....	x
CHAPTER I INTRODUCTION .....	1
CHAPTER II LITERATURE REVIEW .....	3
Cholangiocyte and Function.....	3
Cholangiocyte development, iPSC-derived model, and markers .....	5
Cholangiocarcinoma .....	9
SMAD4 and Role of SMAD4 .....	11
Role of SMAD4 in Hepatocellular carcinoma (HCC).....	13
Role of SMAD4 in Cholangiocarcinoma (CCA).....	13
Role of SMAD4 in other cancers.....	15
Current cholangiocarcinoma models .....	16
3D Cholangiocyte organoids .....	18
CRISPR-CAS9 genome editing.....	19
CHAPTER III MATERIALS AND METHODS.....	21
Human iPSCs culture and maintenance .....	21

Differentiation of iPSC-derived hepatoblasts, cholangiocyte progenitors and cholangiocytes .....	21
Expansion medium (Liver maintenance medium) and selection medium .....	22
Rhodamine 123 uptake assay.....	23
Generation of Inducible <i>SMAD4</i> knockout cassette.....	23
AAVS1-targeted site validation.....	24
Doxycycline treatment.....	24
T7 endonuclease assay.....	24
RNA extraction and Quantitative real-time RT-PCR (qRT-PCR) .....	25
Genomic DNA extraction.....	25
Immunofluorescence .....	26
pGEM-T easy vector cloning .....	26
Organoid formation and quantification of organoid.....	26
Statistical analysis.....	27
CHAPTER IV RESULTS.....	28
Optimize differentiation protocol for generating cholangiocyte progenitor cell using iPSCs.....	28
SMAD4-KO was successfully generated with vary efficiency in any stage of cholangiocyte differentiation using inducible-Cas9-U6-SMAD4 SgRNA iPSC.....	40
Loss of SMAD4 promote iPSC-derived cholangiocyte organoids proliferation survival after low dose radiation .....	48
CHAPTER V DISCUSSION .....	59
REFERENCES.....	62
VITA .....	72

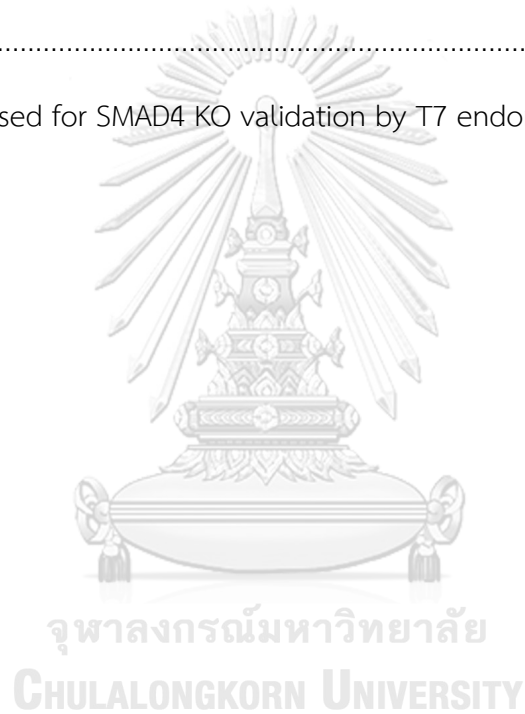




จุฬาลงกรณ์มหาวิทยาลัย  
**CHULALONGKORN UNIVERSITY**

## LIST OF TABLES

	Page
Table 1 Growth factors used in each stage of cholangiocyte differentiation protocol	7
Table 2 Bipotent hepatocytic progenitor, hepatocyte and cholangiocyte Markers.....	9
Table 3 Current cholangiocarcinoma models .....	17
Table 4 Media and growth factors used in each stage of cholangiocyte differentiation .....	22
Table 5 Primers used for SMAD4 KO validation by T7 endonuclease assay .....	25



## LIST OF FIGURES

	Page
Figure 1 Cholangiocyte morphology. ....	4
Figure 2 Anatomical of CCA. ....	10
Figure 3 Immunopathological mechanism of <i>O. viverrini</i> -related CCA. ....	11
Figure 4 Domain structure of SMAD4. ....	12
Figure 5 Signaling pathway involved in SMAD4. ....	12
Figure 6 SMAD4 mutation pattern in biliary tract cancer. ....	14
Figure 7 CRISPR-CAS9 genome editing mechanism. ....	19
Figure 8 Characterization of iPSC-derived cholangiocyte-like cells. ....	30
Figure 9 Characterization of iPSC-derived cholangiocyte organoids. ....	32
Figure 10 Expression of cholangiocyte associated genes and function in iPSC-derived cholangiocyte organoids. ....	34
Figure 11 Differentiation potential of iPSC-derived cholangiocyte organoids. ....	40
Figure 12 Generation of inducible SMAD4 knockout cassette in iPSCs. ....	42
Figure 13 Validation of inducible SMAD4 knockout cassette in iPSCs. ....	44
Figure 14 Characterization of inducible SMAD4 KO iPSC-derived cholangiocyte-like cells and iPSC-derived cholangiocyte organoids and iPSC-derived cholangiocyte lineage-committed cells. ....	48
Figure 15 Validation and TGF- $\beta$ transduction of SMAD4 KO iPSC-derived cholangiocyte organoids. ....	51
Figure 16 Proliferation rate of SMAD4 KO iPSC-derived cholangiocyte organoids. ....	54
Figure 17 Cell viability and the expression of p53 and p21 in SMAD4 KO iPSC-derived cholangiocyte organoids after irradiation. ....	56

Figure 18 Differentiation of mature cholangiocyte of SMAD4 KO iPSC-derived  
cholangiocyte organoids.....57



# CHAPTER I

## INTRODUCTION

Cholangiocarcinoma (CCA), malignancies of the biliary duct system, is a major public health problem especially in the region of northeastern Thailand and increased in several part of the world. Unfortunately, this aggressive cancer was often detected at advanced state with the poor prognosis. To developing cancer therapy, the understanding of the carcinogenesis-involved key pathway mechanism is still needed. Although, the number of mutated tumor suppressor and oncogenic genes have been identified in this cancer, the mechanisms of crucial mutation that drive cholangiocarcinogenesis remain unknown.

SMAD4, a crucial mediator of TGF- $\beta$  signaling pathway, has been linked to *Opisthorchis viverrini* infection associated-intrahepatic CCA with high mutation frequency. (1) In animal models, several studies revealed loss of SMAD4 contribute to carcinogenesis in other cancer type. (2) However, how SMAD4 loss drive to CCA is remain unclear. As mentioned above, early event in CCA development is mostly associated with chronic inflammation such as PSC, recurrent cholangitis, liver cirrhosis and infection with parasite (*ex. Opisthorchis viverrini*). In addition to cholangiocyte, cholangiocyte progenitor is involved in regeneration and homeostasis in chronic inflammation environment. (3) It has been reported that progenitor may serve as the cell origin of CCA. (4-7) However, liver cell contains plasticity. it is still under debate the cellular origin of CCA.

The essential of cancer study is reliable cancer model with resemble human tumor biology. Cancer cell lines are widely used as a tool for cancer study, drug screening and development of new therapies. Due to the loss of the natural cancer heterogeneity and genotypic- phenotypic drift, their mutation and genomic instability of cell lines are limited for studying cancer development. For isolated primary cells, the major limitation is an ethical issue. Recently, human induced pluripotent stem cells (iPSCs) are easy to genetically modified and dividing indefinitely, provide an alternative unlimited cell source for disease modelling. Therefore, iPSC-derived

model may represent as a suitable model for elucidating the molecular mechanisms of cholangiocarcinogenesis.

In this study, we modified culture medium for long-term expansion of iPSC-derived cholangiocyte organoids and generated an inducible *SMAD4* knockout (KO) iPSCs by using TALENs to target inducible *SMAD4* knockout cassette into *AAVS1*, safe harbor site. We demonstrated inducible *SMAD4* KO-iPSCs revealed the potential of dsDNA break at *SMAD4* after doxycycline induction as well as cholangiocyte differentiation potential. Additionally, *SMAD4* KO iPSC-derived cholangiocyte organoids showed increased proliferation rate, reduced irradiation response and defect in tube morphogenesis. Our *SMAD4* KO model will be used as CCA model and still need to investigate the cholangiocarcinogenesis role in further study in vivo.

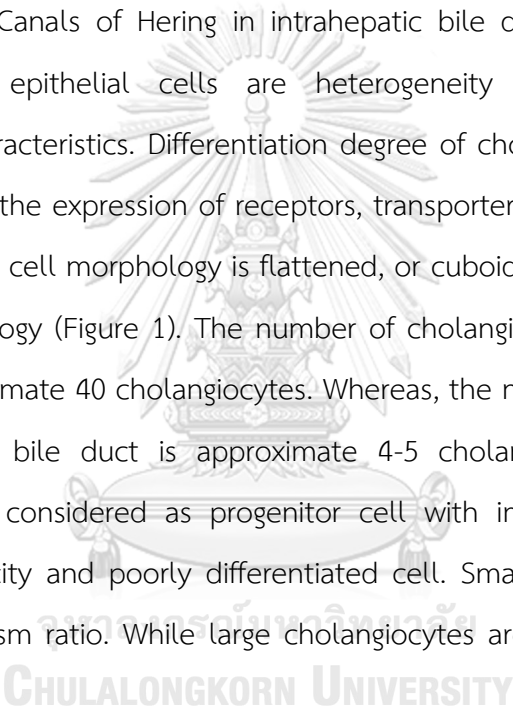


## CHAPTER II

### LITERATURE REVIEW

#### Cholangiocyte and Function

Cholangiocytes, the bile duct epithelial cells, are approximate 3% of liver cell population. Bile duct is divided into Intrahepatic bile duct (within the liver) and extrahepatic bile duct (outside the liver). The tube network of bile duct epithelial cell is start from Canals of Hering in intrahepatic bile duct to duodenum. These continuous duct epithelial cells are heterogeneity in functions, size, and morphological characteristics. Differentiation degree of cholangiocyte (small to large bile duct) is affect the expression of receptors, transporters, and several proteins. (8) In small bile ducts, cell morphology is flattened, or cuboidal and large bile ducts are columnar morphology (Figure 1). The number of cholangiocyte in large intrahepatic bile duct is approximate 40 cholangiocytes. Whereas, the number of cholangiocyte in small intrahepatic bile duct is approximate 4-5 cholangiocytes. (9) Intrahepatic cholangiocyte are considered as progenitor cell with immature characteristics in regeneration capacity and poorly differentiated cell. Small cholangiocytes are high nucleus-to-cytoplasm ratio. While large cholangiocytes are small nucleus with high cytoplasmic area.



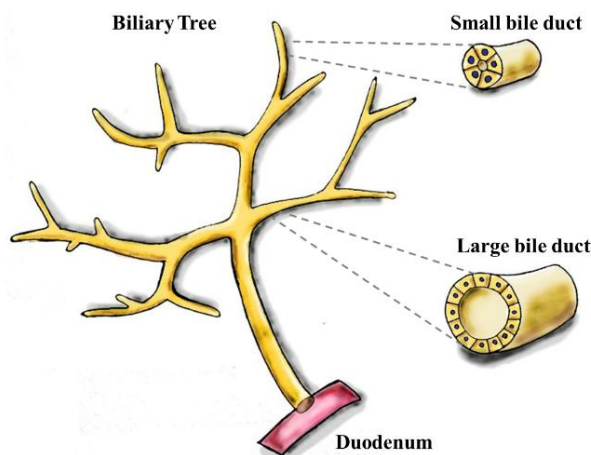


**Figure 1** Cholangiocyte morphology.

The function of cholangiocyte are involved in ion exchanger, bicarbonate secretion, bile acid absorption, water transporter and ductal bile formation. Many transporter/ receptor proteins expressed in cholangiocyte. Apical membrane transporter proteins are involved in liver homeostasis, bile acid modification, bicarbonate secretion (Anion exchanger 2, AE2), water transporter (AQP1, Aquaporin 1), Chloride secretion (cystic fibrosis transmembrane conductance regulator, CFTR), chemo-sensor (G protein-coupled bile acid receptor 1, TGR5), bile acid absorption (apical sodium-dependent bile acid transporter, ASBT). Basolateral membrane transporter proteins are c-AMP activation (secretin receptor, SR), bile absorption (basolateral truncated ASBT, t-ASBT). In addition, intracellular signaling pathway of immature and differentiated cholangiocyte are differently pathway. Both of c-AMP and  $Ca^{2+}$  Signaling pathway are important to bicarbonate and chloride secretion. Immature cholangiocyte which depending on intracellular  $Ca^{2+}$  signaling is considered as hepatic progenitor cell population. However, intracellular c-AMP and  $Ca^{2+}$  signaling are activated in differentiated cholangiocyte. (10) Differentiated cholangiocytes contain cell apico-basolateral polarity and primary cilium. (8)



### Cholangiocyte development, iPSC-derived model, and markers

Since well-understanding of the liver organogenesis studies, the key developmental pathways have been revealed in several reports. (11, 12) The origin of intrahepatic bile ducts is different from extrahepatic bile ducts in term of embryonic development. Intrahepatic bile ducts (IHBD) are derived from hepatoblast (Hepatic progenitor cells) which developed from cranial part ventral foregut endoderm. While extrahepatic bile ducts (EHBD) are directly derived from caudal part of ventral foregut endoderm. The high level of Nodal/TGF- $\beta$  signaling induce the segregation of definitive endoderm from mesoderm. The optimal level of Bone morphogenetic protein (BMP) and WNT signaling pathways support the definitive endoderm differentiation. The Nodal, BMP4, Fibroblast growth factor (FGF) signaling pathways are induce the hepatic specification stage. Hepatic specification provides the foregut progenitor cells which contain multipotent differentiation potential into pancreatic or hepatic commitment. Bipotent hepato-cholangiocyte progenitor (hepatoblast) is located on Canals of Hering of intrahepatic biliary tree which can differentiate into hepatocytes and cholangiocytes. (9) Following cholangiocyte specification, hepatoblasts adjacent the periportal mesenchymal cells are formed single layer of ductal plate and eventually the morphogenesis of intrahepatic bile duct. The expression of cholangiocyte associated genes are upregulated at this stage, while hepatocyte associated genes are downregulated. (13) Wnt, Notch, TGF- $\beta$  and FGF signaling pathway are contribute to cholangiocyte differentiation. Notch signaling play a crucial role in differentiation and morphogenesis of cholangiocyte. (11) Remaining hepatoblast which distant from the portal tract are differentiate into hepatocyte.

As described above, cholangiocyte membrane transporters and its functions are commonly used for cholangiocyte identification. Since the advent of induced pluripotent stem cells (iPSCs), several studies revealed the differentiation protocol of pluripotent cells to hepatic lineage especially PSC-derived hepatocytes. (14-19) In

contrast to the well-known study of hepatocyte differentiation, the iPSC-derived cholangiocyte protocol was later published. Several cholangiocyte differentiation protocols are based on the developmental study of bile duct (Table 1). (11, 12, 20-23) Dianat's protocol was the first cholangiocyte differentiation from iPSC. Growth hormone (GH), epidermal growth factor (EGF), and IL-6 were used in differentiation media. The transporter markers of cholangiocyte including cystic fibrosis transmembrane conductance regulator (CFTR), secretin receptor (SR), ASBT apical sodium-dependent bile acid transporter (ASBT) were expressed. It also formed apicobasal polarity cyst morphology. The combination of OP9 cells with iPSC-derived hepatoblast was cultured by Ogawa's protocol. TGF- $\beta$ , EGF, and HGF were used in cholangiocyte differentiation media. The co-culture technique induces the branch morphology and functional cholangiocyte. This protocol was focused on the notch signaling which crucial for cholangiocyte development and tubulogenesis. While Thiago's protocol was using TGF- $\beta$  alone to drive cholangiocyte maturation. Sampaziotis's protocol was using Activin A, FGF10, and retinoic acid (RA) then EGF was used to induce of cholangiocyte maturation. Many cholangiocyte-specific transporters are expressed in iPSC-derived cholangiocyte including response to hormonal stimulation. Both of Ogawa and Sampaziotis's protocol can generate functional cholangiocyte and disease modeling. However, the current limitation of iPSC-derived cholangiocyte model is fetal gene expression. (22)

**Table 1** Growth factors used in each stage of cholangiocyte differentiation protocol

Protocol	Culture system	Growth Factor Used						CLC
		PSC	DE	HE/HS	HB	HB aggregates* /CP		
Dianat et al., 2014	2D (gelatin, collagen I)	Activin A, FGF2	Activin A, LY294002, WNT3A	Activin A, BMP4, FGF2	HGF, FGF4, EGF, RA	-		GH, IL-6, EGF,
	3D (matrigel)	-	-	-	-	-		HGF, EGF
Ogawa et al., 2015	2D (matrigel, OP9)	FGF2	Activin A, CHIR99021	BMP4, FGF2	Dex, OSM, HGF	Dex, OSM, HGF*		TGF- $\beta$ , HGF, EGF
	3D (matrigel, collagen I, OP9)	FGF2	Activin A, CHIR99021	BMP4, FGF2	Dex, OSM, HGF	Dex, OSM, HGF*		TGF- $\beta$ , HGF, EGF
Thiago et al., 2015	2D (matrigel)	mTesR1	Activin A, WNT3A	BMP4, FGF2, SHH	SHH, Jagged-1	-		TGF- $\beta$
	3D (matrigel, collagen I)	-	-	-	-	-		TGF- $\beta$
Sampaziotis et al., 2015 Sampaziotis et al., 2017	3D (matrigel)	Activin A, FGF2	Activin A, LY294002, FGF2, BMP4, CHIR99021	Activin A	SB431542, BMP4	Activin A, FGF10, RA		EGF

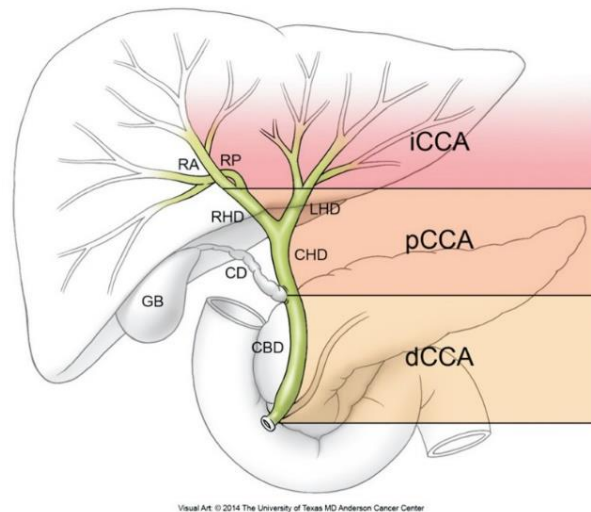
In the current, there is no single specific markers to identify the differentiation of bipotent progenitor cells, immature and mature IHBD. It is still needed several hepto-biliary specific markers. To characterize, the most of cholangiocyte markers are obtained from the studies of animal models and primary human specimens. LifeMap Discovery™ database and Carpino revealed markers to distinguish the hepato-biliary cells (Table 2). (24) Oncostatin M receptor (OSMR), CK7, CK19, DLK-1, ALB, AFP, SOX9, NCAM are expressed in bipotent progenitor cells. SOX9, CK19, OC-1, OC-2, NOTCH2, TGFBR11, SALL4 are expressed in immature IHBD. The expression of HNF4A is not detected in immature IHBD. SOX9 is positive for both immature and mature IHBD. TGFBR11 is only expressed in immature but not in mature IHBD. While immature cell markers are overlap with progenitor cells by expressing stem cell markers (EpCAM, SOX9, AFP). The markers of specific transporters commonly used to separate immature and mature cells (CFTR, SCTR, SSTR2, AE2, SCTR, AQP1, AQP4). The single cell RNA sequencing studies of human liver section revealed the specific markers of adult cholangiocyte (CK19, EpCAM). (25, 26) Only identified markers are not sufficient to define the cell type. The combination of specific markers and functional test often use to identify cell type in hepatic lineage.

**Table 2** Bipotent hepatocytic progenitor, hepatocyte and cholangiocyte Markers

Markers	Cell Type				
	Cholangiocyte	Immature cholangiocyte	Bipotent hepatic progenitor	Immature hepatocyte	Hepatocyte
Primary cilium	+	-	-	-	-
CFTR	+	-	-	-	-
SCTR	+	-	-	-	-
CK19	+	+	+	-	-
CK7	+	+	+	-	-
SOX9	-	+	+	-	-
EpCAM	-	+	+	-	-
CD133	-	-	+	-	-
AFP	-	-	+	+	-
ALB	-	-	+	+	+
HNF4A	-	-	-	+	+
ABCB11 (BSEP)	-	-	-	-	+
CYP3A4	-	-	-	-	+

### Cholangiocarcinoma

Cholangiocarcinoma (CCA) is cancer of bile duct system which can be categorized into 3 groups based on anatomical location: Intrahepatic cholangiocarcinoma (iCCA), perihilar (pCCA) and distal common duct (dCCA) (Figure 2). Among three types of cholangiocarcinoma, iCCA types are rare in western countries. However, it has been reported that the incidence rate has increased in Southeast Asia including Thailand. (27) The prognosis is poor due to detection at a late stage. In terms of pathological features, the categorization of CCA includes mass-forming, periductal-infiltrating or intraductal-papillary. Mass-forming pattern is most often observed in iCCA type. However, periductal-infiltrating pattern is observed in pCCA type.



Visual Art: © 2014 The University of Texas MD Anderson Cancer Center

**Figure 2** Anatomical of CCA.(28)

Among many risk factors that causing CCA such as toxic agents, primary sclerosing cholangitis, *Opisthorchis viverrini* or *Clonorchis sinensis* infection, hepatolithiasis, Caroli's disease and Choledochal cysts. *O. viverrini* Infection is crucial risk factor of CCA in Northeast of Thailand. Mechanism of *O. viverrini*-related CCA may involve mechanical activity of parasite (fluke's sucker), immunopathology (inflammation) and secretory molecules from *O. viverrini* (Figure 4). In chronic inflammation, crucial inflammatory cytokine is TGF- $\beta$ . (29) Due to these mechanism, it has been reported that chromosome 1p36, 9p21, 17q13 and 22q12 contains chromosomal instability. (30) Additionally, *O. viverrini* Infection cause genetic alteration. With genetic background of *O. viverrini*-related CCA, the mutation frequencies of *SMAD4* and *TP53* were dramatically higher than those of non-*O. viverrini*-related CCA. (1) Consequently, *O. viverrini* may affect chromosomal and genetic alteration via these mechanisms which provide a specific mutation frequency pattern.

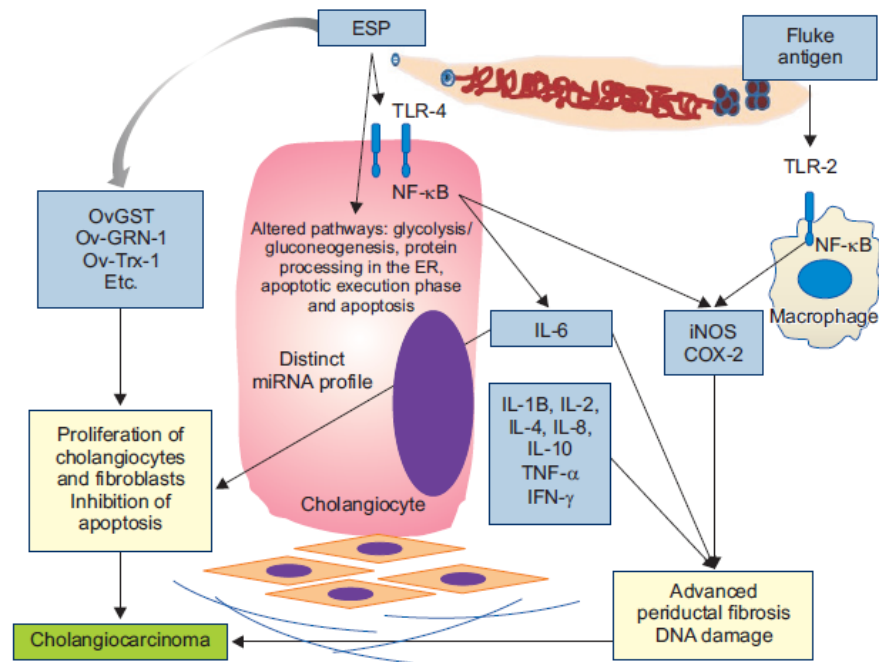


Figure 3 Immunopathological mechanism of *O. viverrini*-related CCA. (29)

#### SMAD4 and Role of SMAD4

SMAD4 gene is encoding SMAD4 protein, which localized on chromosome 18 of long arm at position 21.2 (Figure 4). The SMAD4 protein plays role as a transcription factor and tumor suppressor. Additionally, SMAD4 is also plays role as a central mediator of TGF- $\beta$  and BMP signaling pathway including cell proliferation, cell growth, cell apoptosis, cell differentiation, angiogenesis, and ECM production. In canonical TGF- $\beta$  signaling, TGF- $\beta$  ligand stimulate activation of SMAD2 and SMAD3 via C-terminal phosphorylation by TGF- $\beta$  receptor type I. After that, SMAD Complexes of phosphorylated SMAD2, SMAD3 and SMAD4 translocate into the nucleus and regulate gene expression by interact with DNA transcription factors. In addition, SMAD7 is an essential regulator of canonical TGF- $\beta$  signaling by negative feedback loops. Additionally, SMAD4 is also relate to non-canonical pathway. In the role of MAPK/ERK signaling pathway are cell proliferation and cell survival which can interfere

TGF- $\beta$ /SMAD4 signaling by phosphorylating SMAD2, SMAD3. JNK signaling pathway is involved in cell proliferation and apoptosis. JNK target, C-Jun can bind with corepressor TG-interacting factor to suppress SMAD2 downstream activity. PI3K/AKT signaling pathway which involved in cell proliferation and apoptosis inhibition is suppress phosphorylating SMAD3 via mTOR (Figure 5). (2)

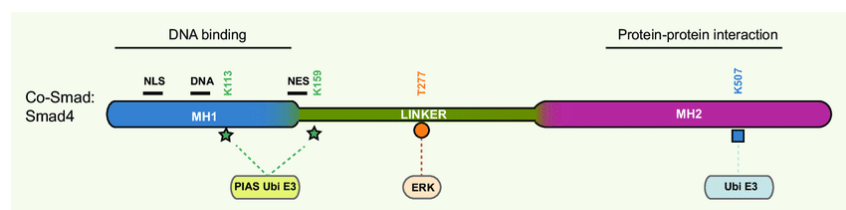


Figure 4 Domain structure of SMAD4. (31)

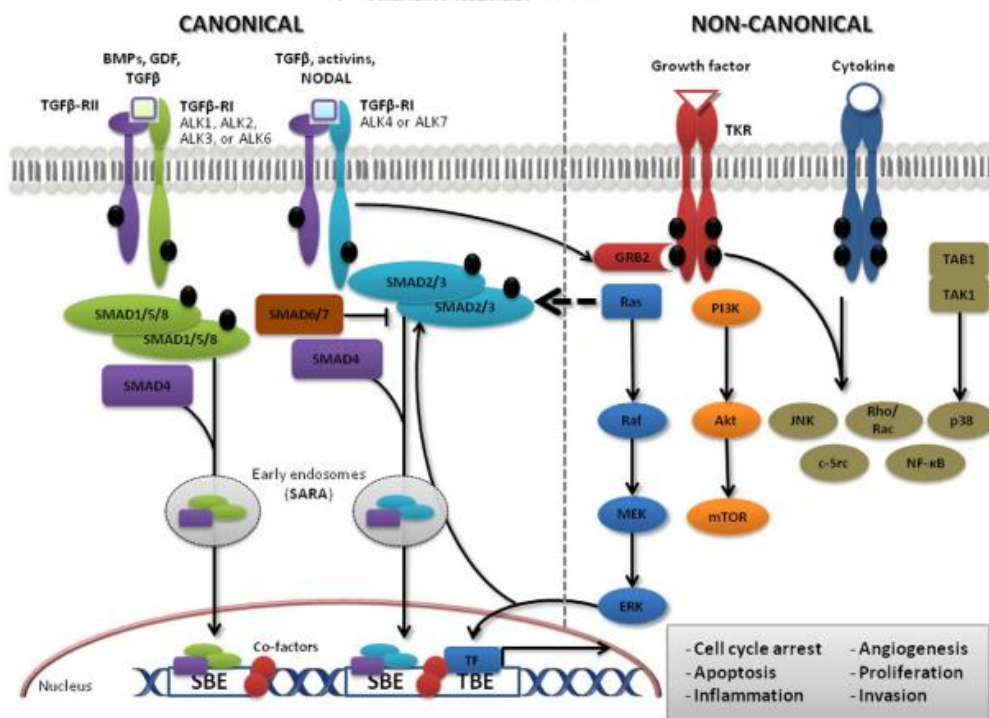


Figure 5 Signaling pathway involved in SMAD4. (32)



### Role of SMAD4 in Hepatocellular carcinoma (HCC)

As crucial mediator of TGF- $\beta$ /BMP signaling pathway, SMAD4 are play role involved in liver regeneration and development. (33) In cholangiocyte commitment, TGF- $\beta$ /SMAD4 signaling are require for cell fate decision of hepatoblast. This signal induce the differentiation of hepatoblast to cholangiocyte. (8) The aberration of TGF- $\beta$ /SMAD4 signaling in hepatoblast generate hybrid hepato-biliary cells. (34)

TGF- $\beta$ /SMAD4 signaling is a proinflammatory cytokine inducing liver fibrosis, cirrhosis, and eventually HCC. In acute inflammation, apoptotic program of hepatocyte is induced by TGF- $\beta$ . Hepatic stellate cell (HSC) are transdifferentiating into myofibroblasts. After chronic inflammation, TGF- $\beta$ /SMAD4 signaling is promote cirrhosis to HCC. The aberration of SMAD4 in HCC are rare and associated with aggressiveness. (33) SMAD4 inhibition is reduce growth and induce apoptotic program of HCC cells. (35) In molecular genomic landscape study in 2018, most frequently mutation of HCC driver genes is involved in *TP53*, *WNT* signaling and *TERT*. While biliary tract cancer driver genes are *TP53*, *ARID1A*, *SMAD4*, *KRAS* and *BAP1*. The role of driver mutation of *SMAD4* is commonly found in biliary tract cancer. It is clear the difference of driver mutation result in CCA and HCC. (36) The most specific gene knockout in mouse models of HCC carcinogenesis are *TP53*, *Wnt/ $\beta$ -catenin*, *c-Myc* and *PTEN*. (37)

### Role of SMAD4 in Cholangiocarcinoma (CCA)

Chronic information from risk factors cause genetic alteration leading to carcinogenesis. The molecular study was pioneered the district mutational profiles of liver fluke-relate and non-liver fluke-related CCA. It was shown that *O. viverrini*-related CCA is predominant with the high mutation frequencies of *SMAD4* (19.4%) in Thailand. It was indicated that the impact of different etiology affects the mutation profiles. (1) In biliary tract cancer, COSMIC (Catalogue of Somatic Mutations in Cancer) database demonstrated that *SMAD4* mutation was often observed in MH1 and MH2

domain but low incident in linker domain (Figure 6). The loss of SMAD4 expression was associated with degree of prognosis in CCA. (38) The various cancer type revealed *SMAD4* mutation. Loss of SMAD4 induce cell proliferation shift from G1 to S phase in cell cycle. (39) It has been demonstrated that TGF- $\beta$ /SMAD4 play important role in EMT in advanced CCA via increased mesenchymal markers. (40) Although loss function of SMAD4 was often found in CCA. (1, 41) It remains unclear in the role of SMAD4 in cholangiocarcinogenesis which arise from cholangiocyte. The role of SMAD4 in cholangiocarcinogenesis remain unknown. Due to difficult to detect at early stage, previous study was proposed cholangiocarcinogenesis model based on histological study with *SMAD4* mutation. (42) Previously, most of carcinogenesis of CCA were studied in genetically engineered mouse models (GEMM) based on Cre-Lox system. It remains unclear conclusion which is a cell origin of CCA, due to not specific cell lineage tracing in liver which may target undesired cell type. (43)

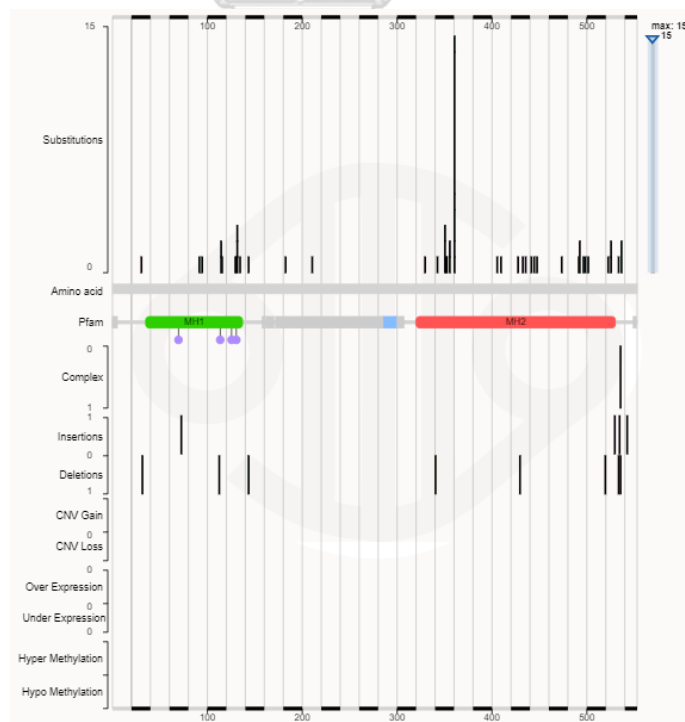


**Figure 6** SMAD4 mutation pattern in biliary tract cancer. (COSMIC)

### Role of SMAD4 in other cancers

In other cancer type, colorectal cancer, the role of SMAD4 are known in colorectal carcinogenesis which contribute to aggressive phenotype and chemoresistance. (44, 45) Loss of SMAD4 alone may contribute to carcinogenesis. Previous study has been reported the role of *SMAD4* in carcinogenesis by using tissue-specific knockout mouse model. The *SMAD4* disruption of animal model can develop to cancer in mammary epithelial cells and epidermal. The disruption of *SMAD4* gene in epithelial cells generating an abnormal characteristic. However, it was not insufficient to tumorigenesis induction in gastrointestinal tract. (2) As an Inflammation-associated cancer, the study of Colitis-associated colorectal cancer revealed the combination of *SMAD4* knockout and chronic inflammation environment can lead to tumorigenesis. (46, 47) Inactivation of SMAD4 is approximately found in 50% of Pancreatic ductal adenocarcinoma (PDAC) patients. In early stage, SMAD4 is play role as tumor suppressor gene which induced cell cycle arrest in cancer cell. (48) Loss of SMAD4 or down-regulated SMAD4 enhanced cancer cell survival from apoptotic program or cell cycle arrest. TGF- $\beta$ /SMAD4 non-canonical pathways (Ras, PI3K, P38 and Rho-GTPase) are dominant in late stage of PDAC. (49, 50) Both of TGF- $\beta$ /SMAD4 canonical and non-canonical pathway can induce aggressiveness of cancer.

### Current cholangiocarcinoma models

The effective CCA models with recapitulate primary cancer are required for the understanding of CCA mechanism and drug screening. It has been reported many CCA model for several years. The most widely used are cell lines. The long-term propagation capacity of cell lines allows to high throughput drug screening study. However, these cells contain genetic alterations and not well characterized in molecular profiles. Most CCA cell lines were obtained from cancer cells accordingly the molecular studies for cancer initiation need to be concerned (Table 3). To date, introducing genetic editing models can result in the molecular study of target gene which allowing to the mechanism understanding of gene. Genetically engineered mouse models (GEMMs) are frequently use for study of target gene alteration (tumor suppressor genes, oncogenes). It has been reported the cholangiocarcinogenesis involved signaling pathway such as Notch, KRAS IDH1 and P53. Several models revealed the mixed CCA-HCC. It should be noted that this model is difficult to determine the molecular mechanism of carcinogenesis at the early stage. To bridge the gap of these limitations, organoids (3D culture system) represent tissue-specific structure with recapitulate human organ. Extracellular matrix (ECM) was used for culture organoids to establish apico-basal polarity. It has been reported the cholangiocarcinogenesis of human liver organoid with combination of SMAD4 and tumor suppressor gene knockout. It was unclear how loss of SMAD4 alone affect to organoid or drive to carcinogenesis.

**Table 3** Current cholangiocarcinoma models

Cholangiocarcinoma models			
Model	Name/ Induction	Characteristic	Reference
Cell lines	MMNK-1	Human Telomerase immortalized cholangiocyte cell line	(51)
	Choi-CK	Human iCCA with abnormality of chromosome 3, 6, 7, 8, 12, 14, 17, and 18	(52)
	SCK	Human iCCA with moderate differentiated cell	(52)
	SNU-1079	Human iCCA with IDH1 heterozygous	(53)
	KKK-D049	Human iCCA with well differentiated cell	(54)
	KKK-D068	Human iCCA with adenosquamous l and contain chromosome Y aberration	(54)
GEMMs	<i>SMAD4-PTEN</i> knockout	Hyperplastic nodule with no cancer progression	(55)
	<i>KRAS</i> knockin / <i>P53</i> knockout	Develop iCCA with metastatic progression	(56)
	<i>P53</i> knockout / $CCl_4$	Develop iCCA with hyperplasia and fibrotic environment	(57)
Organoid	<i>BAP1</i> , <i>TP53</i> , <i>PTEN</i> , <i>SMAD4</i> , and <i>NF1</i> knockout in human liver organoid	Develop human CCA in mice with impaired cell polarity and organization	(58)

### 3D Cholangiocyte organoids

Organoids are *in vitro* 3D culture technology with resemble to real organ structure. It can derive directly from human adult stem cells or pluripotent stem cells. It represents self-renewal and differentiation capacity. The long-term culture of organoid provides stable genotypic and phenotypic characteristic corresponding the original tissue. The protocols of multiple tissue-specific organoid have been established. (59) These organoids can act as a modelling for development and drug screening. Niche factors are the environment which required for organoid maintenance. The niche factor condition in human liver organoid was established in 2015. (60) Based on human intestinal organoid culturing, R-spondin, epidermal growth factor (EGF), WNT3A, HGF, FSK, Gastrin, FGF10, TGF- $\beta$  inhibitor and nicotinamide are required for promoting the long-term expansion of liver organoid.

The developmental study provides required key stages and essential growth factors for organogenesis. Interestingly, the effort of generation of organs in a dish is result in an organoid technology. Organoid culture system is 3D culture *in vitro* system may derive from embryonic stem cell (ESC), induced pluripotent stem cell (iPSC) or derived from adult-progenitor cell. With self-renewal and expansion capacity, their structure resembles *in vivo* tissue structure as mini organ. In case of cholangiocyte-associated disease studies, the ethic of using cholangiocyte primary cells (2-3% of liver cells) lead to find an alternative source. As pluripotent and undifferentiated capacities, ESC is used as unlimited cell source which provides various differentiated-cell type. (61) Previously, there was no reported a functional cholangiocyte differentiation from human pluripotent stem cell until Dianat and colleagues were performed in 2014. (20) However, it was not closely resembled cholangiocyte molecular profiles. Recently, cholangiocyte differentiation protocol was established by using 3D organoid culture system. (22) It shows the cholangiocyte functional properties and specific markers such as GGT1, CFTR, CK7 and SOX9.

Additionally, this cholangiocyte organoid was used to study cholangiocyte specific disease and represented disease's characteristic. (21)

### CRISPR-CAS9 genome editing

Genome editing technologies are efficient method for genome sequences modification. Earlier genome editing approaches, zinc-finger nucleases (ZFNs) and transcription-activator like effector nucleases (TALENs), have limitation in cost, time consuming in large scale studies. As emerging a new nucleases approach in 2013, CRISPR-CAS9 (Clustered Regularly Interspaced Short Palindromic Repeats and CRISPR-associated genes) is the type II CRISPR nuclease system which consist of Cas9, gRNA, crRNA and trRNA. In fundamental mechanism of CRISPR-CAS9, Complex CAS9-gRNA will be generated by trRNA. This complex can bind and cleave target gene. Cleaved target DNA can repair into 2 patterns: Non-homologous End Joining (NHEJ) with base insertion or deletion and Homology directed repair (HDR) with same DNA template (Figure 7). These patterns of DNA repair are necessary for study function of gene. The application of this technology to genome editing in organoids were reported by various specific cell types. (62, 63)

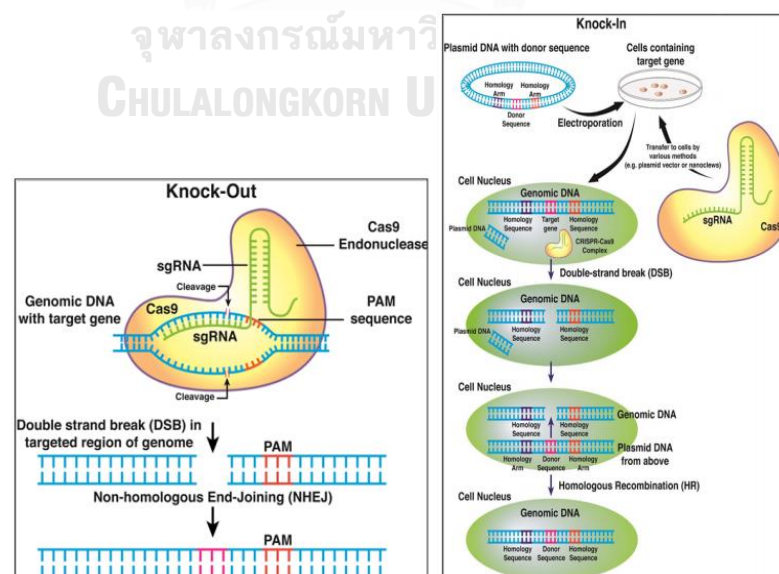


Figure 7 CRISPR-CAS9 genome editing mechanism. (64)

For application in carcinogenesis modelling, it has been reported that CRISPR-CAS9 was used in sequential mutation of human colorectal organoid. (65) Inactivation of *SMAD4* had successful rate with indel mutation. Interestingly, targeted organoid revealed self-selective growth advantage and *in vivo* tumorigenic capacity. Taken together, combination of CRISPR-CAS9 and organoid technology may provide more understanding of cholangiocarcinogenesis mechanism.





## CHAPTER III

### MATERIALS AND METHODS

#### Human iPSCs culture and maintenance

iPSCs were cultured on Matrigel-coated dish with mTeSR1 medium (StemCell Technologies) and dissociated by using CTK enzyme (consist of 10 % collagenase IV, 0.25 % trypsin, 1mM CaCl<sub>2</sub>, H<sub>2</sub>O and 20% knockout serum replacement) when the confluency of cell is up to 80%-90%. iPSCs were incubated at 37° C with 5%CO<sub>2</sub>. Medium was replaced daily.

#### Differentiation of iPSC-derived hepatoblasts, cholangiocyte progenitors and cholangiocytes

Cholangiocyte differentiation protocol was performed as described in Sampaziotis (2017). iPSCs were dissociated into small clumps by using 0.5ml of CTK enzyme. Cells were incubated for 7 minutes at 37°C. Then cells were washed by 1ml of 1x phosphate buffer saline (PBS) for twice. After that, cells were maintained on gelatin-coated plate in chemically defined medium-polyvinyl alcohol (CDM-PVA) medium supplemented with 10 ng/ml activin A and 12 ng/ml FGF2. This day referred as Day 0. The medium was replaced as described in Table 4. To prevent over confluence, cells were dissociated with 1ml of 1x TrypLE™ Select Enzyme at day 7. To differentiate into cholangiocyte-like cell, cholangiocyte progenitor was dissociated and cultured in 3D with Matrigel.  $1 \times 10^6$  cells were mixed with 50% (vol/vol) Matrigel supplemented with 20 ng/ml EGF and 10  $\mu$ M Rho kinase inhibitor (Y-27632) and this mixture was dropped into 6-well plate for 200  $\mu$ l. Cells were incubated for 30 minutes at 37 °C. Medium was replaced every 2 days. Cells at day 26 were referred as cholangiocyte-like cells.

**Table 4** Media and growth factors used in each stage of cholangiocyte differentiation

Stage	Day	Media	Growth factors
Pluripotent	Day 0	CDM-PVA	10 ng/ml activin A 12 ng/ml FGF2
Definitive endoderm	Day 1	CDM-PVA	100 ng/ml activin A 80 ng/ml FGF2 10 ng/ml BMP-4 10 $\mu$ M LY294002 3 $\mu$ M CHIR99021
	Day 2	CDM-PVA	100 ng/ml activin A 80 ng/ml FGF2 10 ng/ml BMP-4 10 $\mu$ M LY294002
	Day 3	RPMI	100 ng/ml activin A 80 ng/ml FGF2
Foregut progenitor	Day 4 - 8	RPMI	50 ng/ml activin A
Hepatoblast	Day 9 - 12	RPMI	10 $\mu$ M SB-431542 50 ng/ml BMP-4
Cholangiocyte progenitor	Day 13 - 16	RPMI	50 ng/ml activin A 50 ng/ml FGF10 3 $\mu$ M retinoic acid
Cholangiocyte-like cells	Day 17 - 26	WE	20 ng/ml EGF

#### Expansion medium (Liver maintenance medium) and selection medium

iPSC-derived cholangiocyte-like cells were maintained in Advanced DMEM/F-12 supplemented with 30% (vol/vol) Rspo1-conditioned medium, 30% (vol/vol) Wnt3a-conditioned medium, 1:100 N2 supplement, 1:50 B27 supplement, 1 mM N-acetylcysteine, 10 mM nicotinamide, 10 nM recombinant human gastrin I, 100 ng/ml recombinant human FGF10, 25 ng/ml recombinant human HGF, 50 ng/ml recombinant human EGF, 5  $\mu$ M A83-01, 10  $\mu$ M Forskolin, and 25 ng/ml Noggin. To

select *SMAD4* KO cholangiocyte organoids, selection medium (liver maintenance without Noggin and A83-01) was used in this study. 10 ng/ml TGF- $\beta$  was added into this medium.

### **Rhodamine 123 uptake assay**

Cholangiocyte organoids were incubated with 100  $\mu$ M rhodamine 123 in Hanks' Balanced Salt solution (HBSS) containing for 10 minutes. Then cholangiocyte organoids were washed three times with HBSS for 5 minutes. For MDR1 inhibition, cells were incubated with 10  $\mu$ M verapamil for 30 minutes before Rhodamine 123 incubation.

### **Generation of Inducible *SMAD4* knockout cassette**

*SMAD4* gRNA was used in this study obtained from Sato (2015). To generate U6 promoter with *SMAD4* gRNA Cassette, *SMAD4* gRNA was cloned into BPK1520 vector followed Joung lab gRNA cloning protocol. A pair of primer which contains homology arm of Puro-Cas9 donor at *SacI* restriction site was designed for amplify U6-*SMAD4* gRNA PCR product. This PCR product was cloned into Puro-Cas9 donor by using In-Fusion HD Cloning Kits (Clontech). An inducible *SMAD4* gRNA cassette was analyzed by DNA sequencing for vector validation.

### **iPSC transfection and selection**

iPSCs were pre-treated with 10  $\mu$ M Y27632 one day before electroporation.  $1 \times 10^6$  cells of iPSCs were dissociated into single cells by using Accutase (Thermo Fisher Scientific). Cells were incubated for 3 minutes at 37°C. mTeSR1 medium was added into cell mixture. Then cell mixture was centrifuged at 800 rpm for 4 minutes. Medium was removed from cell pellet. Cells were resuspended in 100  $\mu$ l of Nucleofection solution P3 which contains 5  $\mu$ g of AAVS1-TALEN-L, 5  $\mu$ g of AAVS1-TALEN-R, 10  $\mu$ g of AAVS1-Neo-M2rtTA and 10  $\mu$ g of *SMAD4* Puro-Cas9 donor. This cell mixture was transferred into nucleofection cuvette and electroporated by 4D-

Nucleofector™ X (Lonza) with CB-150 program. Pre-warm mTeSR1 medium was added into the cell mixture in the nucleofection cuvette. Cells were transferred to new Matrigel-coated plate with mTeSR1 medium and 10  $\mu$ M Y27632. After electroporation, transfected cells were treated with 0.5  $\mu$ g/mL of Puromycin for 3 days, followed by 70  $\mu$ g/mL of geneticin treatment for 5 days. After that, transfected cells were treated with 0.5  $\mu$ g/mL of puromycin and 70  $\mu$ g/mL of Geneticin combination for 6 days. When confluency, each single clone of iPSC was dissociated into Matrigel-coated plate for expansion and validation.

#### **AAVS1-targeted site validation**

To determine AAVS1-target site of vector in iPSC, CAS9-AAVS1 primer and m2rtTA-AAVS1 primer were used for analysis by thermocycler. PCR product was separated by gel electrophoresis.

#### **Doxycycline treatment**

To activate Cas9 activation, cells were treated with doxycycline (2  $\mu$ g/mL, 5  $\mu$ g/mL) for 3 days. Medium was replaced daily. Cells were dissociated for genomic DNA or RNA extraction.

#### **T7 endonuclease assay**

To detect *SMAD4* indel of genomic DNA, 50 ng of genomic DNA was amplified by PCR. PCR products was reannealed by using the following protocol: 95°C, 5 minutes; 95°C–85°C at  $-2^{\circ}\text{C}/\text{s}$ ; 85°C–25°C at  $-0.1^{\circ}\text{C}/\text{s}$ ; hold at 4°C. The hybridized PCR products were incubated with 5U of T7EI (NEB) at 37°C for 15 minutes and analyzed with gel electrophoresis. Intensity of product band was determined by ImageJ.

**Table 5** Primers used for SMAD4 KO validation by T7 endonuclease assay

Primers	Sequence
SMAD4#2T7_F	TTAATCCAGTTGTTTTGGGTGC
SMAD4#2T7_R	ACACCGACAATTAAGATGGAGTG

### RNA extraction and Quantitative real-time RT-PCR (qRT-PCR)

Total RNA was extracted RNA by using TRI Reagent®. The collected cells were resuspended in TRI Reagent for 10 minutes. 200 µl of BCP solution was mixed into cell mixture and incubated for 10 minutes at room temperature. Then this cell mixture was centrifuged at 12,000 rpm for 10 minutes at 4°C. Clear aqueous phase was transferred into new tube. Isopropanol was added into this tube and incubated at 4°C for overnight. After centrifugation, mixture was washed twice with 70% ethanol. The RNA pellets were dissolved with nuclease-free water. cDNA was synthesized by using RevertAid™ H Minus Reverse. qRT-PCR was performed using Maxima SYBR Green/ROX qPCR Master Mix (2X) on Biosystems 7500 Fast Real-Time PCR system (Applied Biosystems). qRT-PCR primers of cholangiocyte differentiation was obtained from Sampaziotis (2015). qRT-PCR primer of Cas9 fragment was obtained from Gonzalez (2014). *GAPDH* was used as internal control housekeeping gene.

### Genomic DNA extraction

Genomic DNA was extracted using the DNeasy Blood & Tissue Kit (Qiagen). Briefly, pellet cells were resuspended in 1xPBS. 20 µl of Proteinase K solution and 200 µl of AL solution were added into cell mixture. Then the cell mixture was incubated in heating block at 56°C for 10 minutes. Absolute ethanol was added into the cell mixture. The cell mixture was transferred to column and centrifuged at 8,000 rpm for 3 minutes. Then it was washed and centrifugated. Genomic DNA was eluted with nuclease-free water. Concentration of genomic DNA was measured by spectrophotometer.

### **Immunofluorescence**

Cells were fixed in 4% paraformaldehyde in PBS for 20 minutes at room temperature. Cells were permeabilized and blocked with blocking buffer solution (2% BSA, 0.3% Triton X-100 in PBS or 2% BSA in PBS) for 1 hour at room temperature. Next, the cells were incubated at 4 °C for overnight with the following primary antibodies diluted in antibody diluent solution. Cells were washed three times with 0.05% Tween 20 in PBS for 5 minutes and incubated for 2 hours at room temperature with secondary antibodies in antibody diluent solution. Cells were washed three times with 0.05% Tween 20 in PBS for 5 minutes. Nuclei were stained using 4',6-diamidino-2-phenylindole (DAPI) (1:1000) for 5 minutes. Cells were washed three times with PBS for 5 minutes each and then imaged using a fluorescence microscope.

### **pGEM-T easy vector cloning**

*SMAD4* fragment was amplified by using PCR. The amplified *SMAD4* fragment was purified by using QIAquick Gel Extraction Kit. The purified *SMAD4* fragment was cloned into pGEM-T easy vector (Promega) and incubated at 4°C for overnight. This plasmid DNA was transformed into competent cells and extracted for genomic DNA sequencing analysis.

### **Organoid formation and quantification of organoid**

Organoids were dissociated into single cells by TrypLE select enzyme. 1,000 cells were mixed with 10% Matrigel and seeded into 96-well plate. Cells (whole-well image) were counted for colonies at day 1 and day 4 after seeding. The quantification of organoids was measured and analyzed with ZEISS ZEN Microscope Software.

### **Organoid irradiated-induced DNA damage**

Single cells (100,000 cells) were cultured in 70% Matrigel and seeded into 12-well plate. Organoids were treated with X-ray radiation (2 days after seeding). Dose of

radiation vary between 0 – 8 Gy for optimal concentration. Cells were collected at 96 hours after irradiation for cell survival analysis (CellTiter-Glo™). For p53 and p21 mRNA expression, cells were collected for RNA extraction at 24h and 48h after irradiation and analyzed by RT-PCR.

### Statistical analysis

T-test statistical analysis was performed by using GraphPad Prism (GraphPad Prism 8.4.0).



## CHAPTER IV

### RESULTS

#### Optimize differentiation protocol for generating cholangiocyte progenitor cell using iPSCs

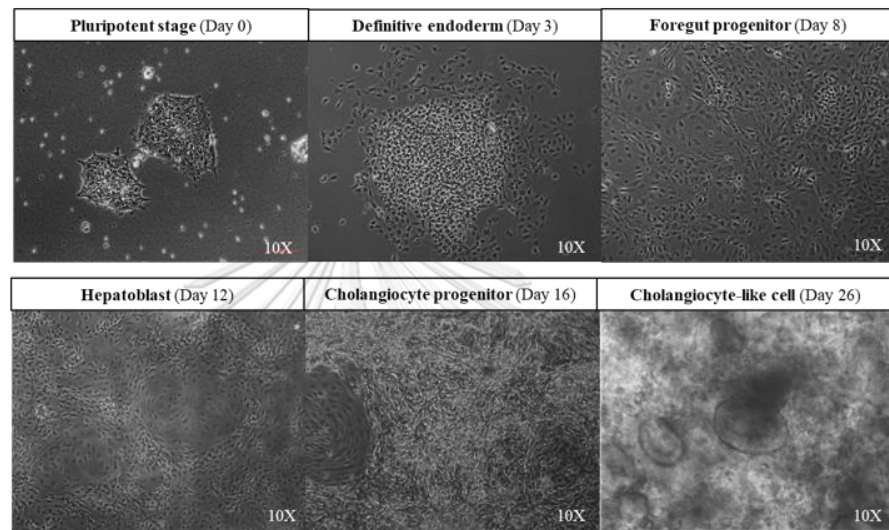
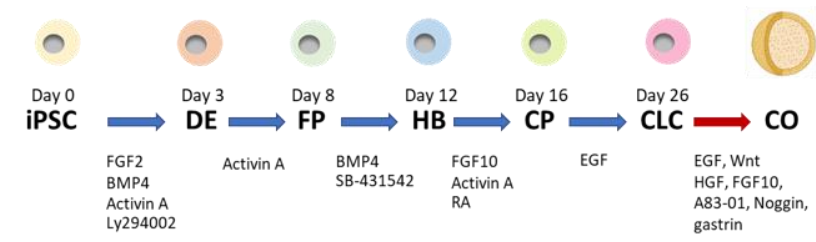
Recently, iPSC-derived cholangiocyte differentiation protocols were developed in order to generate mature cell for drug testing and modeling biliary disorder. (22) Due to the interline variability, we first validated published cholangiocyte differentiation protocol using our iPSC (Figure 8A, upper panel).

iPSCs were stepwise differentiated into definitive endoderm (SOX17<sup>+</sup>), foregut progenitor cells (FOXA2<sup>+</sup>), and hepatoblast (HNF4A and CK19 positive cells) which are the precursor of hepatocytes and cholangiocytes. For cholangiocyte specification, hepatoblast were cultured in differentiation medium supplemented with fibroblast growth factor 10 (FGF 10). 4 days after culture, SOX9<sup>+</sup>CK19<sup>+</sup> cells, cholangiocyte progenitor cells, were observed, and then terminally differentiated into 3D structure cholangiocyte-like cells (CLCs) by culture in Matrigel (Figure 8A and B).

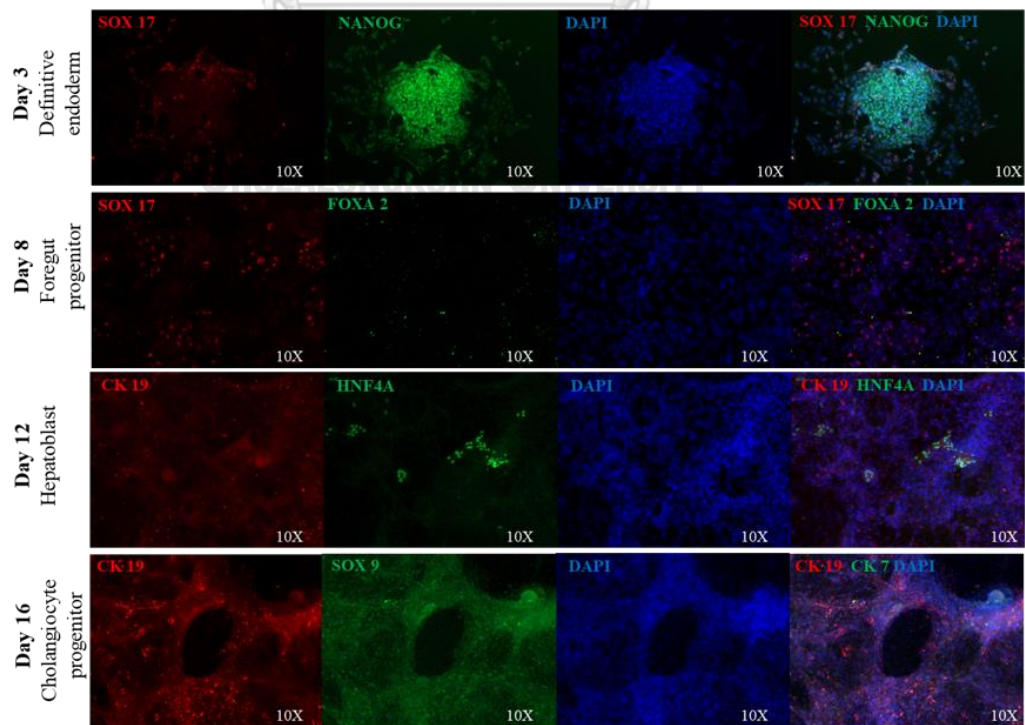
iPSC derived CLCs expressed cholangiocyte specific markers (*CK19*, *CK7*) (Figure 8C). However, these CLCs have a limit expansion potential which cannot be subculture and generate large number of cells for large scale experiment. To overcome this limitation, we modified CLC culture media by adding growth factors, gastrin I, FGF10, hepatocyte growth factor (HGF), epidermal growth factor (EGF), A83-01, Noggin that have been known to support cholangiocyte proliferation. (60) We called these cells as iPSC-derived cholangiocyte organoids.



A



B



C

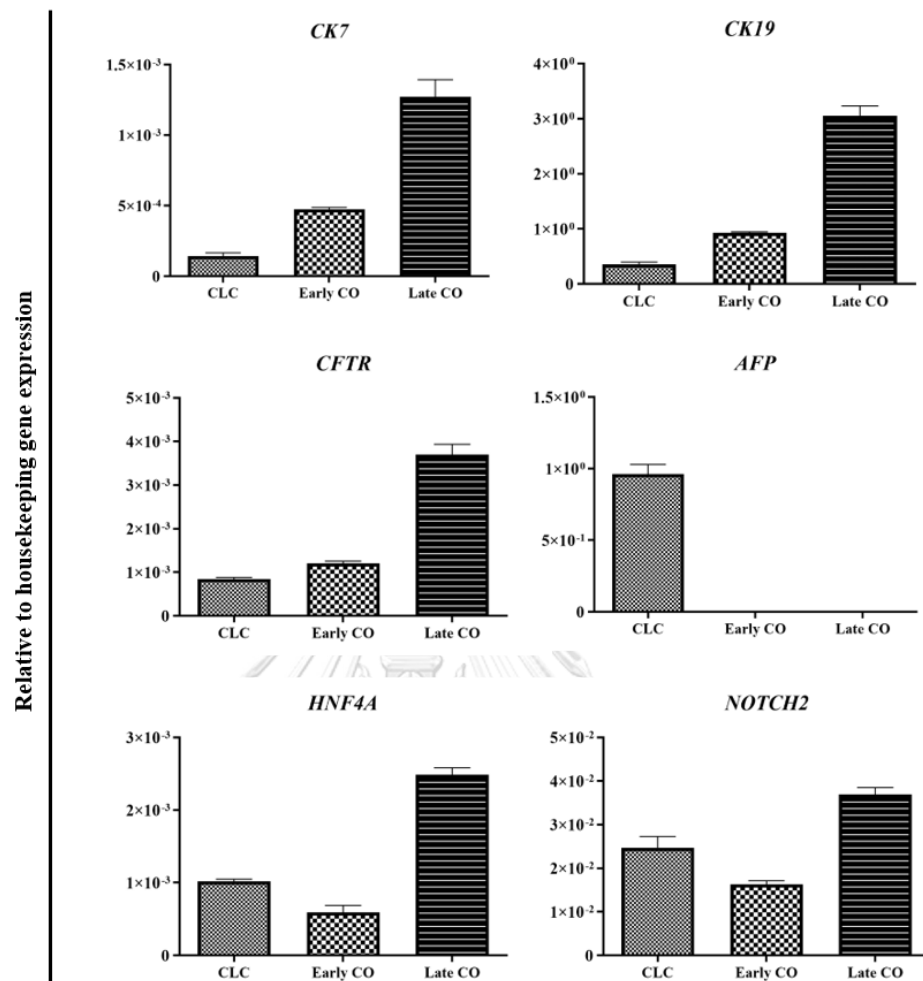
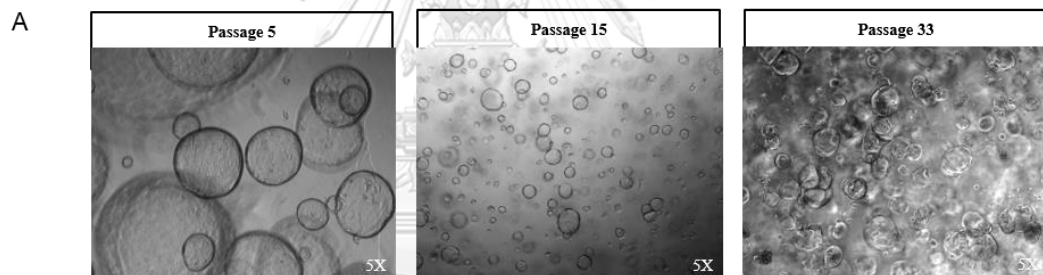


**Figure 8** Characterization of iPSC-derived cholangiocyte-like cells.

(A) Differentiation timeline of cholangiocyte organoids derived from CLCs modified from study of Huch (2015), Sampaziotis (2017) and Light microscopy images and (B) Immunofluorescence images of cholangiocyte differentiation. (C) Quantitative real-time RT-PCR (qRT-PCR) analysis of cholangiocyte-associated genes in iPSC-derived cholangiocyte-like cells (CLC), iPSC-derived cholangiocyte organoids (CO) at early (P.4) and late passage (P.18). n = 3 biological replicates for each sample. iPSC; induced pluripotent stem cell; DE, definitive endoderm; FP, foregut progenitor cell; HB, hepatoblasts; CP, cholangiocyte progenitors; CLC; cholangiocyte-like cells; CO, iPSC-derived cholangiocyte organoids; Early CO, iPSC-derived cholangiocyte organoid passage 5; Late CO, iPSC-derived cholangiocyte organoid passage 18, *CK7*, cytokeratin 7; *CK19*, cytokeratin 19; *AFP*, alpha fetoprotein; *CFTR*, cystic fibrosis transmembrane conductance regulator; *HNF4A*, Hepatocyte nuclear factor 4 alpha. The relative expression levels were compared to the house keeping gene, Glyceraldehyde 3-phosphate dehydrogenase (*GAPDH*).

iPSC-derived cholangiocyte organoids showed better proliferation potential as these cells can be long-term cultured for more than 8 months (Figure 9A). iPSC-derived cholangiocyte organoids expressed cholangiocyte specific markers (CK19, CK7, SOX9) and negative for hepatocyte markers (AFP, ALB) (Figure 9B). Compare to CLCs, cholangiocyte progenitor marker, *CK19*, was upregulated in iPSC-derived cholangiocyte organoid as well as others cholangiocyte mature marker *CK7* and *CFTR*. The expression of mature hepatocyte marker, *AFP*, was reduced while *HNF4A*, regulator of hepatocyte differentiation was not different (Figure 8C). These results suggesting that CLCs acquired more cholangiocyte characteristics and might retain the potential of hepatocyte differentiation after culture in our expansion media. Moreover, this expression of cholangiocyte specific genes was slightly increased during long-term culture of iPSC-derived cholangiocyte organoids.



B

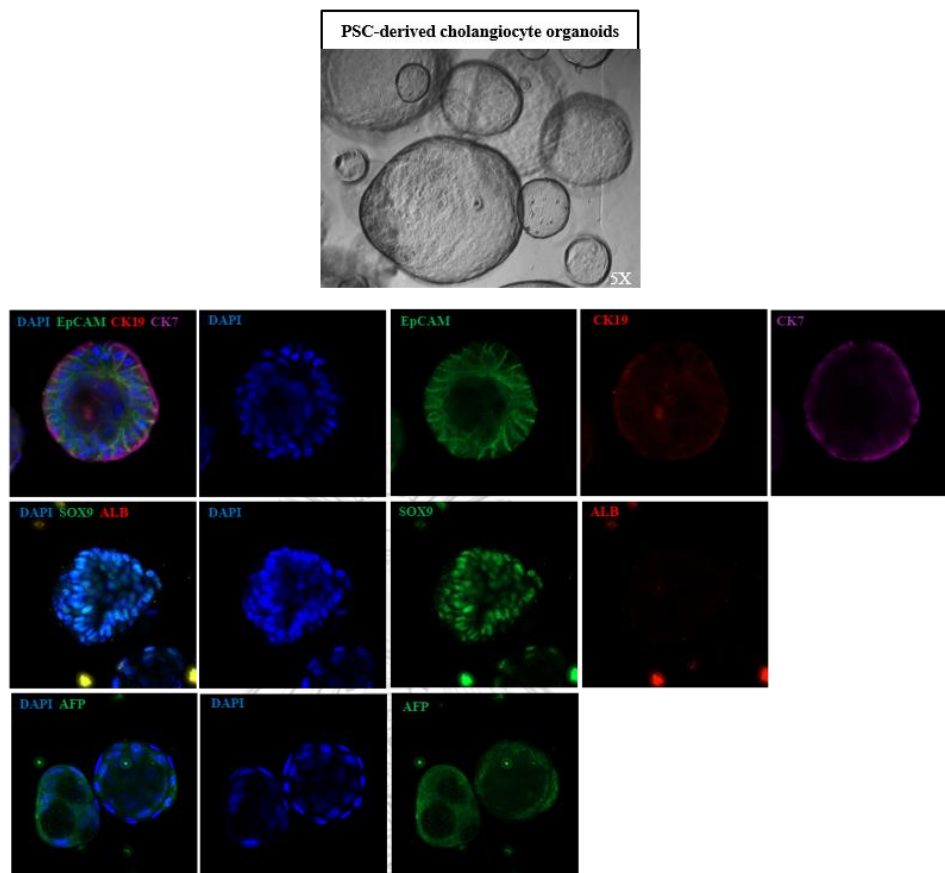


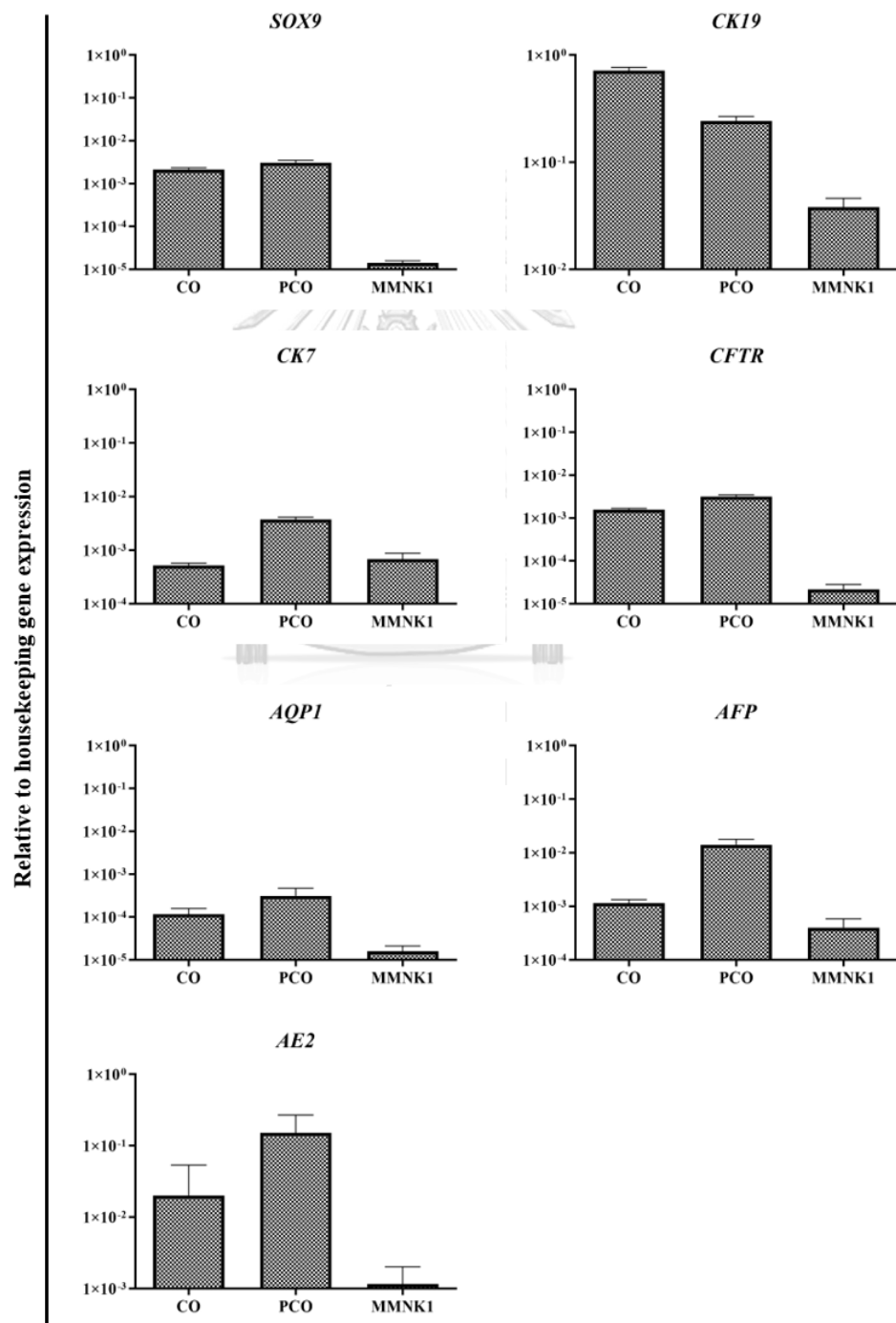
**Figure 9** Characterization of iPSC-derived cholangiocyte organoids.

(A) Light microscopy images of iPSC-derived cholangiocyte organoids at passage 5, 15, and 33. (B) Light microscopy and immunofluorescence images of iPSC-derived cholangiocyte organoids.

Next, we tested whether iPSC-derived cholangiocyte organoids resemble to primary cholangiocytes isolated from adult liver. RT-PCR revealed the expression level of cholangiocyte specific markers, *CK19*, *CK7*, *SOX9*, *AFP*, *CFTR*, *AQP1* and *AE2* in iPSC-derived cholangiocyte organoids were more comparable to primary cholangiocyte organoids than MMNK-1, mostly used cholangiocyte cell line (Figure 10A). The important physiological function of cholangiocyte is transportation of small substances, to modulate bile composition by MDR1 transporter. To determine the functionality of MDR1, iPSC-derived cholangiocyte organoids were cultured in the presence of Rhodamine 123, MDR1 substrate, and transportation of Rhodamine 123 was observed 20 minutes after incubation using fluorescence microscopy. The

fluorescence of Rhodamine 123 was detected inside the lumen of iPSC-derived cholangiocyte organoids which indicate the transportation of Rhodamine 123 from the basal (outside) to the apical (inside) side. Additionally, in the presence of Verapamil, MDR inhibitor, the transportation into the central lumen was inhibited (Figure 10B).

A



B

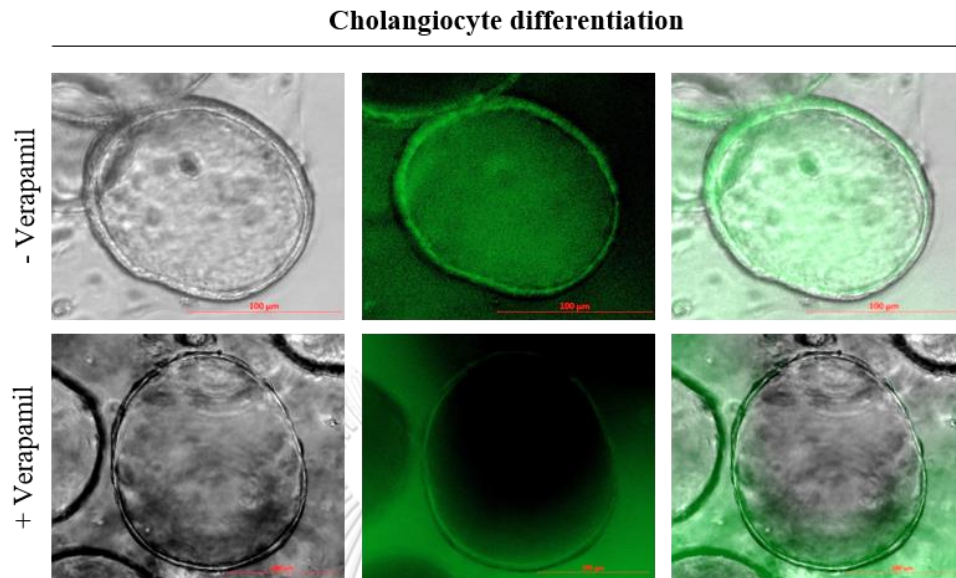


**Figure 10** Expression of cholangiocyte associated genes and function in iPSC-derived cholangiocyte organoids.

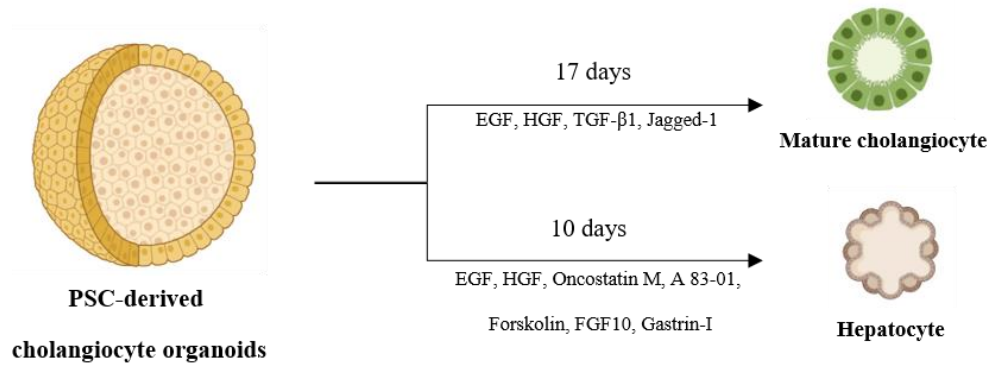
(A) Quantitative real-time RT-PCR (qRT-PCR) analysis of cholangiocyte-associated genes and cholangiocyte-specific transporters in iPSC-derived cholangiocyte organoids compare to primary organoids from adult cells and MMNK-1. (B) Rhodamine 123 uptake of iPSC-derived cholangiocyte organoids with (lower panel) or without Verapamil (upper panel). CO, iPSC-derived cholangiocyte organoid; PCO, primary cholangiocyte organoid; MMNK1, immortalized human cholangiocyte cell line; *CFTR*, cystic fibrosis transmembrane conductance regulator; *ASBT*, apical sodium-dependent bile acid transporter; *AQP1*, aquaporin 1; *AE2*, anion exchange protein 2 ; *SSTR2*, somatostatin receptor 2; *SOX9*, SRY-Box transcription factor 9.

Biliary tubulogenesis is the critical state for bile duct development. We next ask whether iPSC-derived cholangiocyte organoids have ability to form tubular structure. HGF, EGF, TGF- $\beta$ 1 and Notch signaling have been known as key factors that promote tubular morphogenesis. (23) In the presence of these signaling, iPSC-derived cholangiocyte organoids developed extended structures that resemble to tubular morphology which branched and elongated corresponding to the day of differentiation (Figure 11A). Mature cholangiocyte markers, *CK7*, *ASBT*, *AE2*, *AQP1*, and *SSTR2*, was significantly increased in differentiated cells compare to cholangiocyte

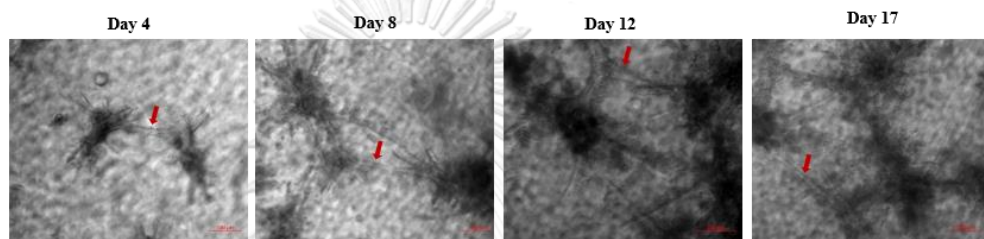
organoid. (Figure 11B). These results indicated that iPSC-derived cholangiocyte organoid displayed cholangiocyte characteristic and functional in vitro. Nonetheless, the remaining of fetal gene expression, such as *LIN28B*, was observed in iPSC-derived cholangiocyte organoids (Figure 11C). There are many studies reported that, during recovery phase after liver injury, biliary epithelial cell has ability to transdifferentiated into hepatocyte to restore the loss of parenchymal mass. So, we next test whether iPSC-derived cholangiocyte organoids have hepatocyte function.

When cultured with hepatocyte differentiation media, morphology of iPSC-derived cholangiocyte organoids were changed from cyst structure with central lumen to compact spheroid (Figure 11D). RT-PCR analysis demonstrated the downregulation of cholangiocyte specific genes, *CK17*, *CK19* and significantly upregulation of gene that found in functional hepatocytes including *CYP34A*, *ALB*, *MRP2*, *TAT* and *CYP2C9* in hepatocyte differentiated cells (Figure 11E). ALB positive cells were detected by immunofluorescence staining. This finding indicated that iPSC-derived cholangiocyte organoids have a potential to differentiate into hepatocyte-like cells (Figure 11D). Together with data, our modified cholangiocyte differentiation protocol could generate functional iPSC-derived cholangiocyte organoids that have long-term expansion potential which can generate large number of cholangiocyte for biliary disease modeling and drug testing.

A

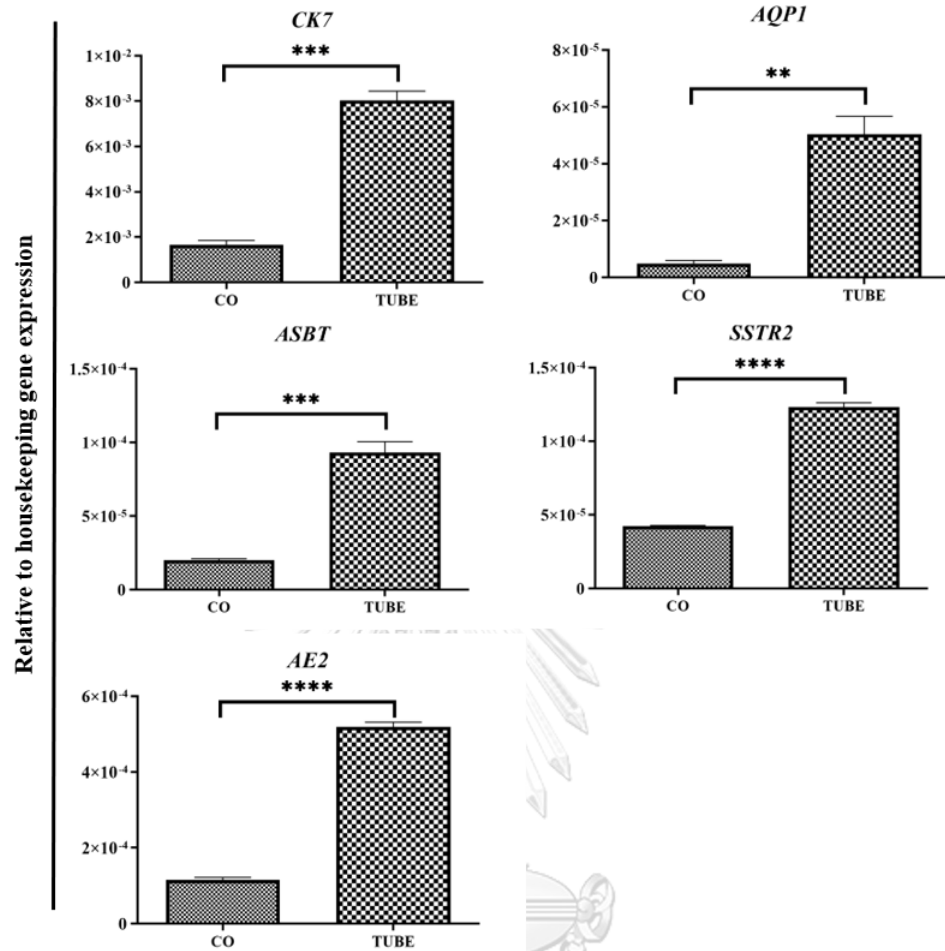


### Cholangiocyte differentiation

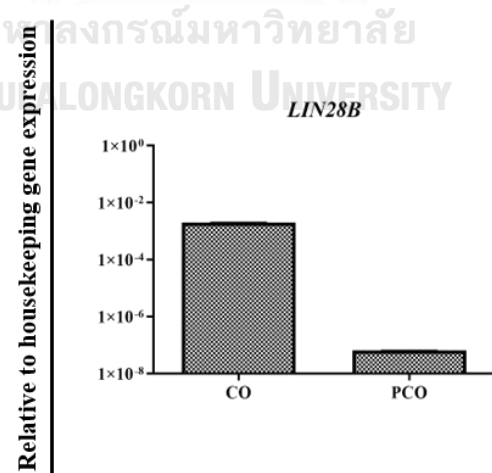




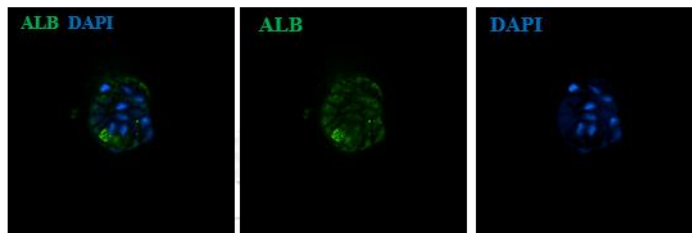
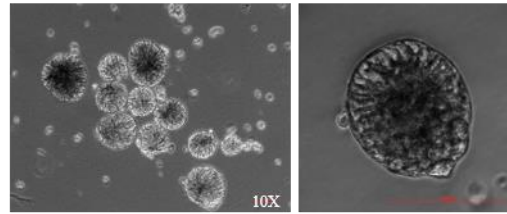
B



C



D

**Hepatocyte differentiation**

E

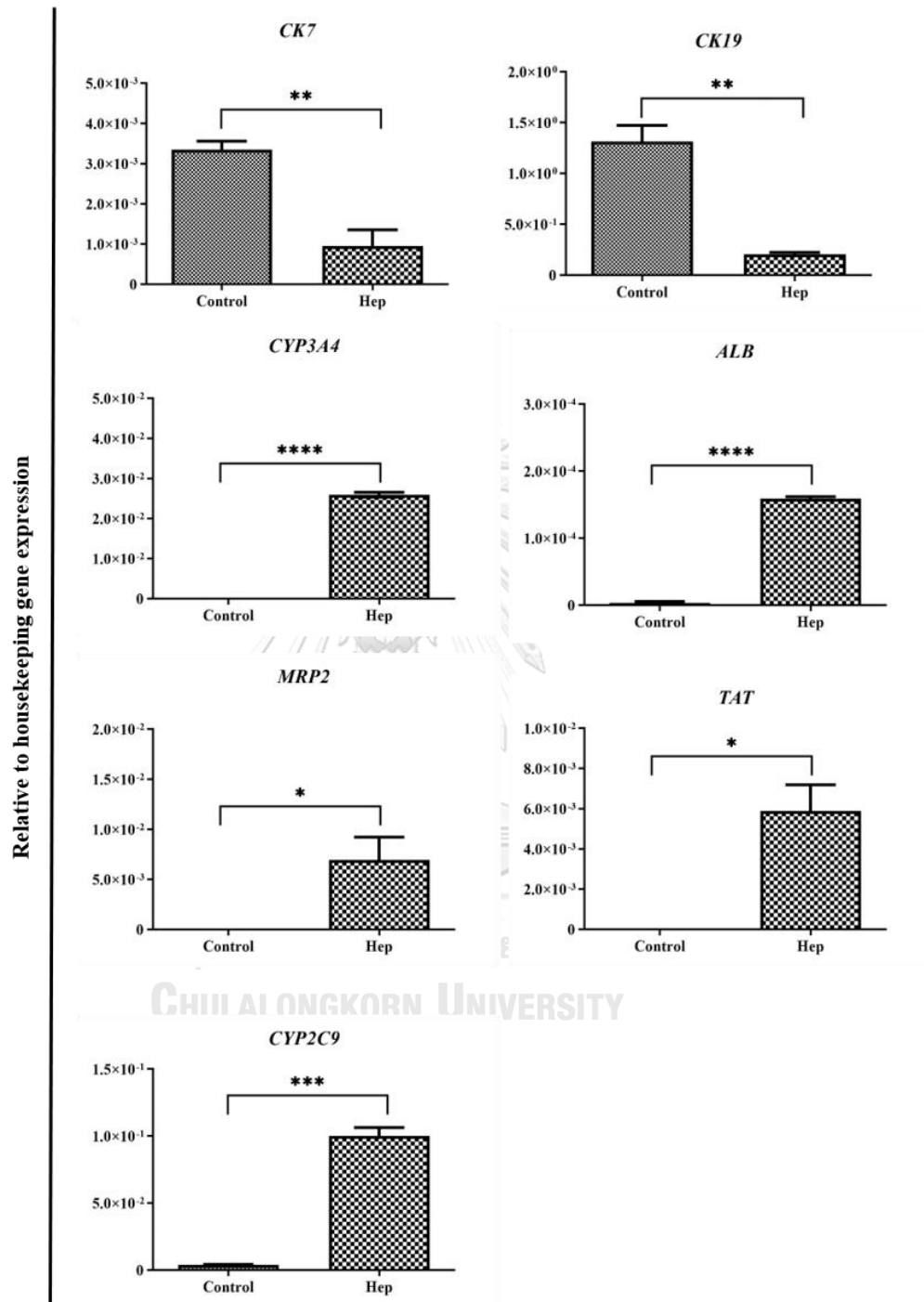


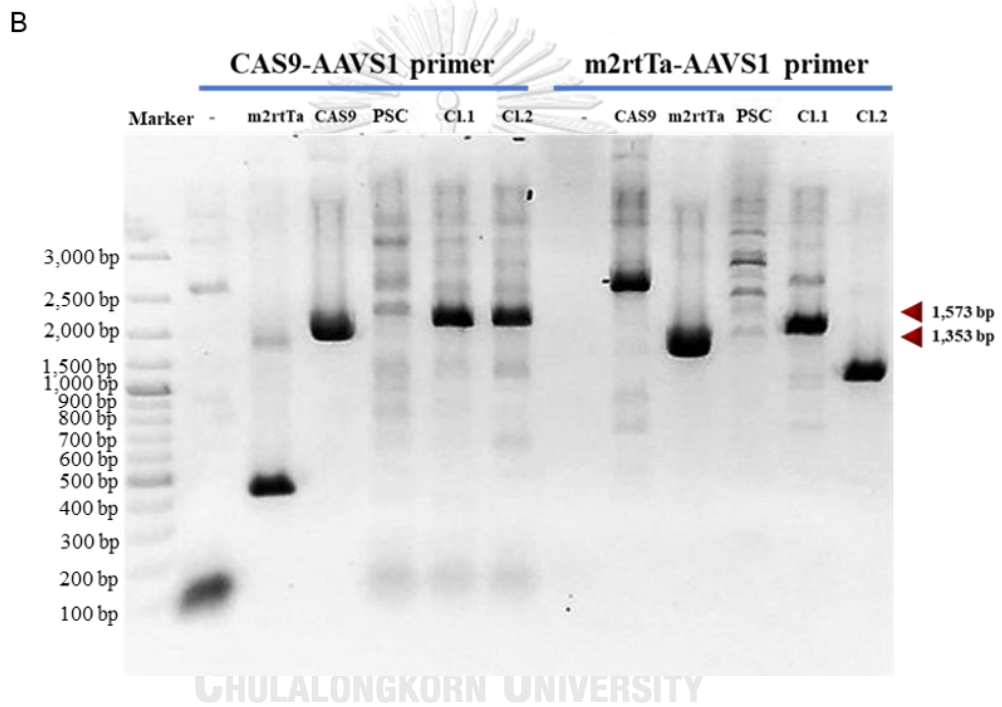
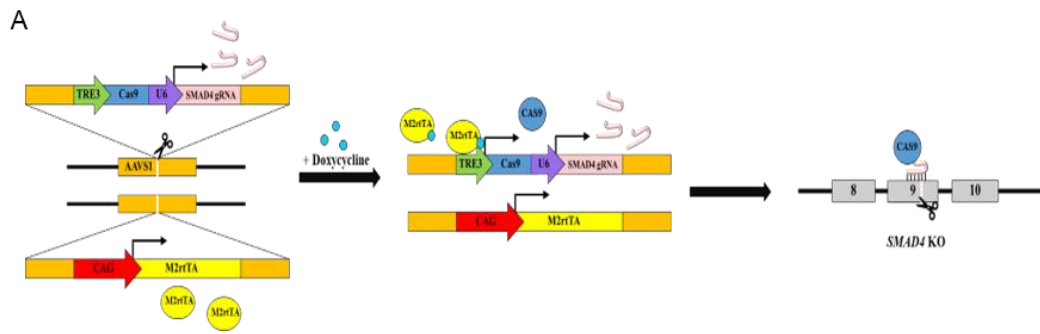
**Figure 11** Differentiation potential of iPSC-derived cholangiocyte organoids.

(A) cholangiocyte and hepatocyte differentiation protocol outline and brightfield images of tube morphogenesis of iPSC-derived cholangiocyte organoids. (B) RT-PCR of cholangiocyte-specific genes and transporter genes in tube formation differentiation compare to cholangiocyte organoids. (C) qRT-PCR analysis of fetal gene (*LIN28B*) expression in iPSC-derived cholangiocyte organoids compare to primary organoids. (D) Light microscopy and immunofluorescence images of hepatocyte differentiation. (E) qRT-PCR analysis of cholangiocyte-associated genes and mature hepatocyte-associated genes in hepatocyte differentiated cells. Red arrow indicates duct-like structure. Co or Control, iPSC-derived cholangiocyte organoid; PCO, primary cholangiocyte organoid; Hep; Hepatocyte-induced cholangiocyte organoids; TUBE, cholangiocyte organoids in tube formation medium, *CYP3A4*, cytochrome P450 3A4 ; *ALB*, albumin ; *MRP2*, multidrug resistance-associated protein 2; *TAT*, tyrosine aminotransferase; *CYP2C9*, cytochrome P450 2C9; *LIN28B*, Lin-28 Homolog B.

### **SMAD4-KO was successfully generated with vary efficiency in any stage of cholangiocyte differentiation using inducible-Cas9-U6-SMAD4 SgRNA iPSC**

SMAD4 is a key mediator of TGF- $\beta$  and BMP signaling which play a critical in development as well as differentiation of mature cholangiocyte. In order to elucidate the role of SMAD4 in cholangiocarcinoma using iPSC-derived cells, Dox-inducible CRISPR/Cas9 system was used to knockout *SMAD4* at specific stage during iPSC to cholangiocyte differentiation.

SgRNA targeted *SMAD4* at V370 position (65), which is a conserved and MH2 domain that essential for TGF- $\beta$  and BMP signaling transduction, was synthesized, and cloned into inducible Cas9 vector (66) under the control of U6 promoter in order to generate Dox-inducible *Cas9-U6-SMAD4* SgRNA cassette. Dox-inducible and rtTA cassette were specifically targeted into *AAVS1* locus (Safe harbor) of iPSC through homologous recombination using TALEN (Figure 12A). Inducible-*Cas9-U6-SMAD4* SgRNA iPSC (in*SMAD4*-KO iPSC) were selected by using puromycin and geneticin. The presence of inducible cassette and rtTA cassette of *AAVS1* locus of the selected clone were confirmed by PCR (Figure 12B and C). Moreover, this iPSC still express NANOG, OCT4 which confirmed their pluripotency (Figure 12D).



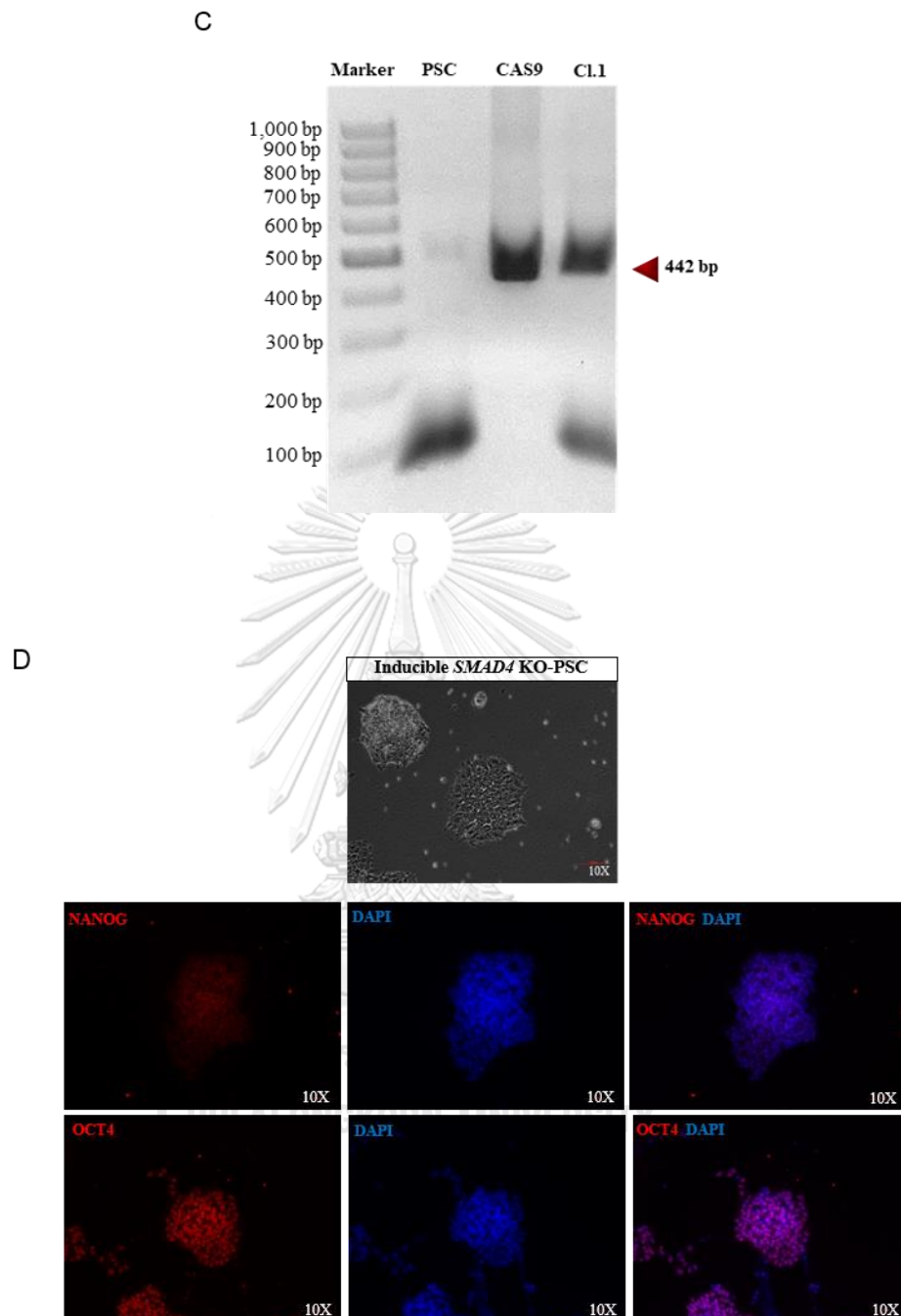
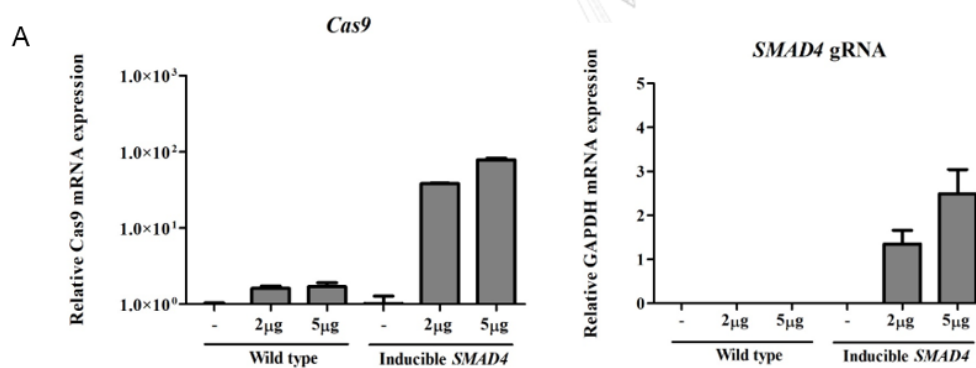


**Figure 12** Generation of inducible *SMAD4* knockout cassette in iPSCs.

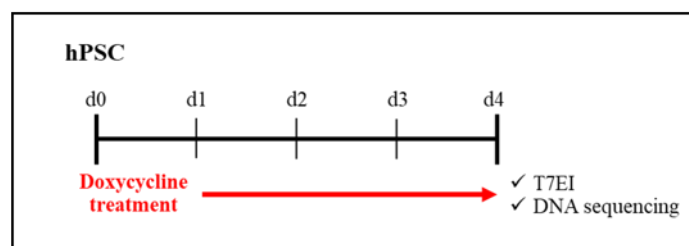
(A) TALEN-mediated gene targeting of an inducible *SMAD4* knockout cassette and Neo-m2rtTA into *AAVS1* locus. Induced *Cas9* expression with doxycycline treatment result in DNA double-strand break (DSB) in *SMAD4* target gene. (B) PCR analysis of *AAVS1*-target site of inducible *SMAD4* knockout vector and m2rtTA vector. (C) PCR analysis of *SMAD4* gRNA part (U6 promoter-*SMAD4*

gRNA-guide scaffold) which is crucial part of inducible *SMAD4* knockout vector. (D) Light microscopy image and immunofluorescence of in*SMAD4*-KO iPSCs.

To validate the CRISPR/ Cas9 inducible system, in*SMAD4*-KO-iPSCs were treated with doxycycline for 72 hours. qRT-PCR analysis revealed the upregulation of *CAS9* and *SMAD4*-SgRNA expression upon doxycycline treatment (Figure 13A). Next, we test whether this inducible system could introduce mutation in *SMAD4* gene. in*SMAD4*-KO iPSCs were treated with 2  $\mu\text{g}/\text{ml}$  doxycycline for 72 hours and T7 endonucleases I (T7EI) mismatch detection assay was used to evaluate indel mutation rate (Figure 13B). 20 % indel mutation rate was detected in in*SMAD4*-KO iPSC treated with doxycycline (Figure 13C). DNA sequencing of *SMAD4* gene indicated frameshift mutation pattern which confirmed the knockout efficiency of the inducible system in pluripotent state (Figure 13D).



**B**



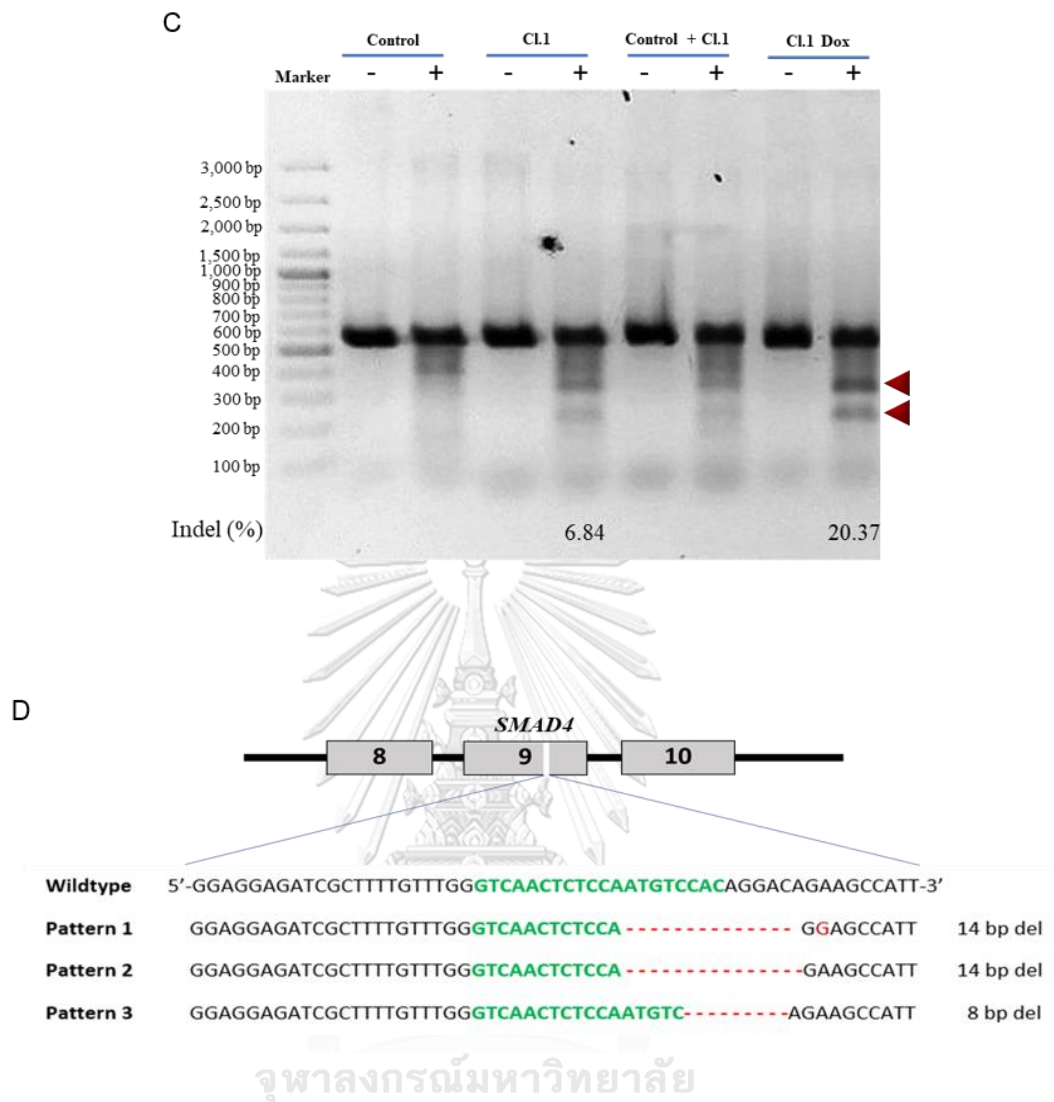


**Figure 13** Validation of inducible SMAD4 knockout cassette in iPSCs.

(A) Quantitative real-time RT-PCR (qRT-PCR) analysis of *Cas9* expression and SgRNA expression with or without doxycycline treatment in inSMAD4-KO iPSC (B) Timeline of doxycycline treatment in inSMAD4-KO iPSC (C) T7 endonuclease I mismatch detection of SMAD4 gene knockout at PSC stage. In this study, red arrowhead indicate the expected T7E1-specific fragments used to quantify indel frequency. (D) Representative sequence patterns of various knockout mutant clones. Control or Wildtype, SMAD4 Wildtype-iPSCs; CL1, inSMAD4-KO clone 1.

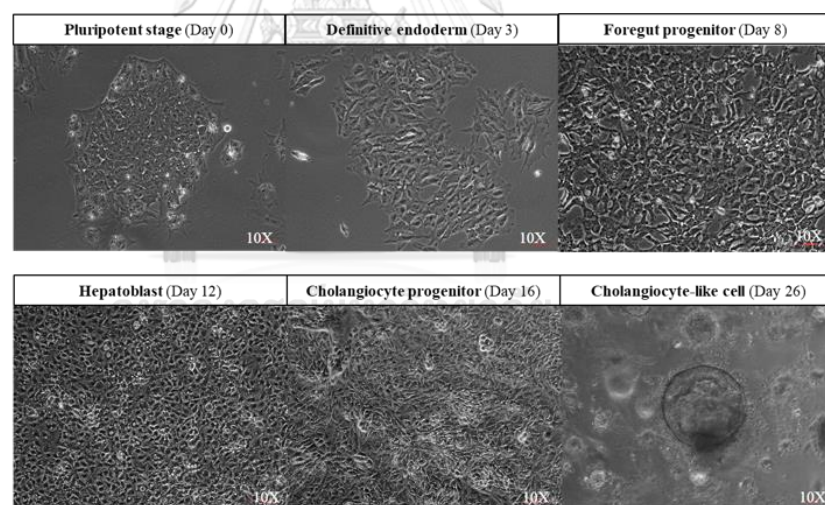
To determine the SMAD4-KO efficiency in each stage of cholangiocyte differentiation, inSMAD4-KO iPSCs were stepwise differentiated as described above (Figure 14A, B and C). SMAD-KO efficiency in hepatoblast stage and cholangiocyte



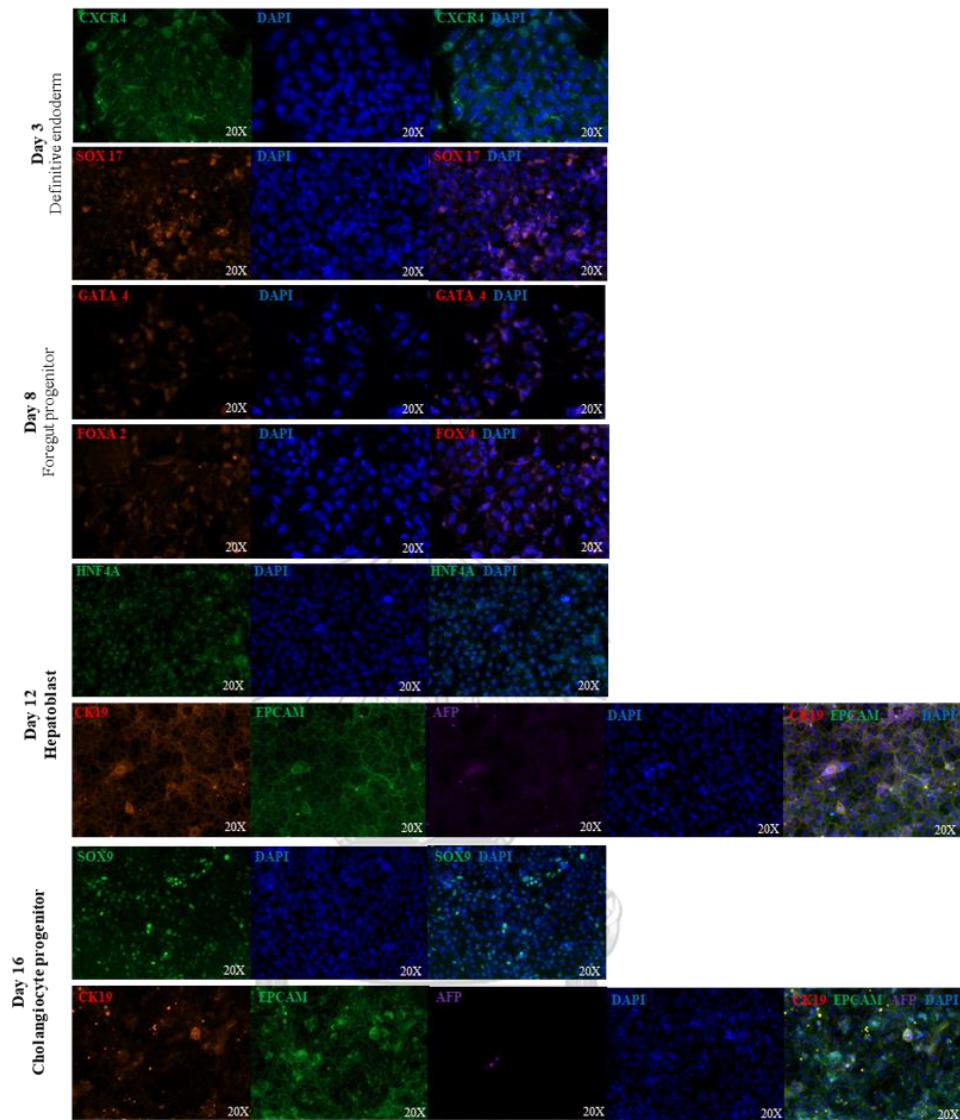
progenitor state were analyzed 72 hours after additional of doxycycline (Figure 14D). Indel mutation rate was gradually decreased during differentiation. 5.6% and 4.26% indel were detected in hepatoblast and cholangiocyte progenitor, respectively, after treatment with 2  $\mu\text{g}/\text{ml}$  doxycycline (Figure 14E and F). Increase the doxycycline concentration to 5  $\mu\text{g}/\text{ml}$  could enhanced *SMAD4* mutation efficiency. However, high concentration of doxycycline affected both iPSC and cholangiocyte cell growth. Thus, 2  $\mu\text{g}/\text{ml}$  doxycycline was used in further experiment.

These results demonstrated that our in*SMAD4*-KO iPSC is a useful tool for studying the role of SMAD4 signaling in each stage of cholangiocyte, as well as cholangiocarcinoma development. Moreover, this iPSC line can be use to modeling the role of SMAD4 in other cell type that has successful iPSC differentiation protocol.

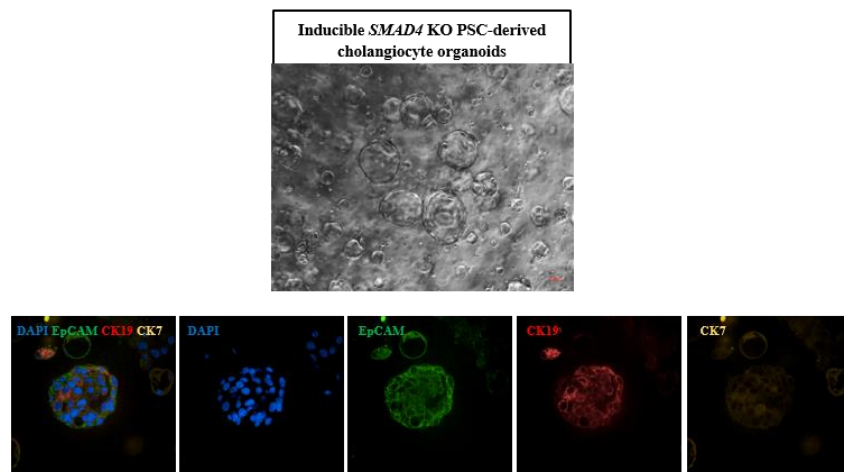
A



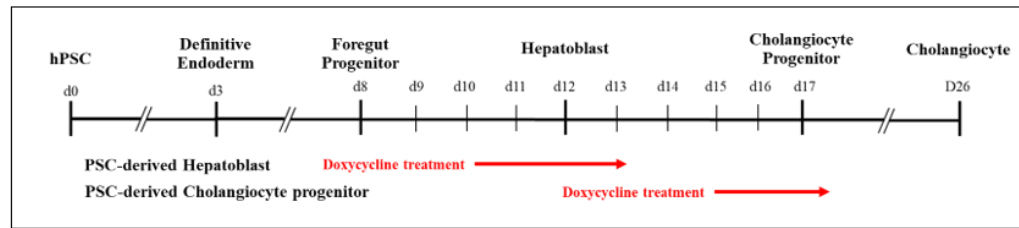
B



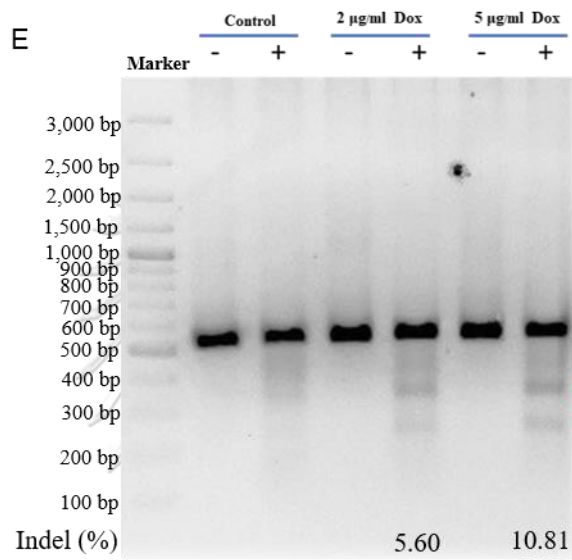
C



D



E



F

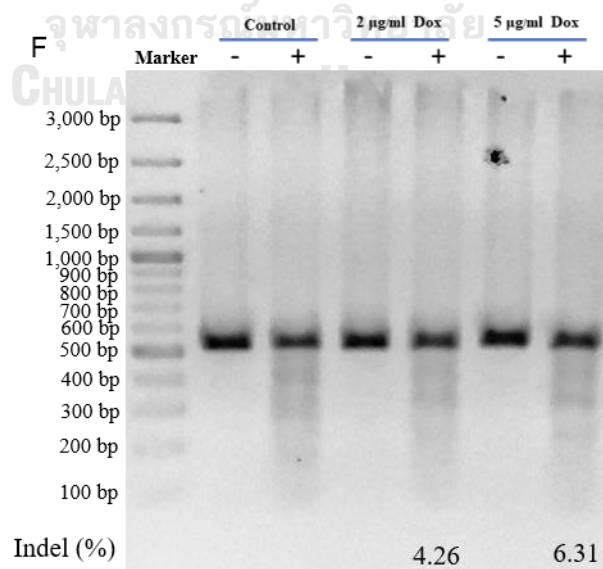


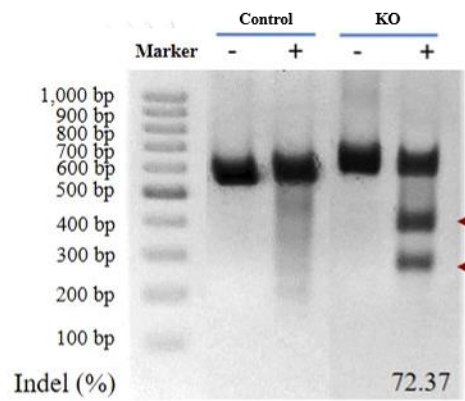
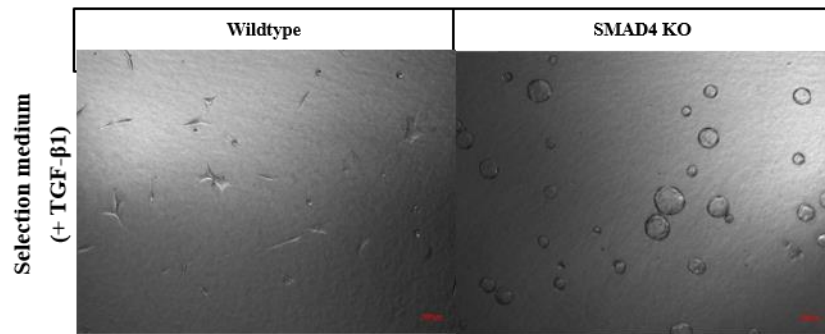
**Figure 14** Characterization of inducible *SMAD4* KO iPSC-derived cholangiocyte-like cells and iPSC-derived cholangiocyte organoids and iPSC-derived cholangiocyte lineage-committed cells. (A) Light microscopy images and (B) immunofluorescence images of cholangiocyte differentiation. (C) Bright field and immunofluorescence images of inducible *SMAD4* KO iPSC-derived cholangiocyte organoids. (D) Timeline of doxycycline treatment in cholangiocyte lineage-committed cells; hepatoblasts, cholangiocyte progenitors. (E) T7 endonuclease I mismatch detection of *SMAD4* gene knockout at hepatoblast stage. (F) T7 endonuclease I mismatch detection of *SMAD4* gene knockout at cholangiocyte progenitor stage. In this study red arrowhead indicates the expected T7EI-specific fragments used to quantify Indel frequency.

### **Loss of SMAD4 promote iPSC-derived cholangiocyte organoids proliferation survival after low dose radiation**

To assess *SMAD4* function, iPSC-derived cholangiocyte organoids were treated with doxycycline for 5 days. Dox-induced cholangiocyte organoids were cultured in expansion media supplemented with TGF- $\beta$ 1 in order to selected *SMAD4*-derived cholangiocyte organoid (Figure 15A). After selection, *SMAD4* KO-iPSC derived cholangiocyte organoids were cultured and expanded in expansion media without noggin and A83-01. TE7I assay revealed indel mutation at *SMAD4* gene. DNA sequencing showed 21 bp and 5 bp deletion in MH2 domain which confirmed the knockout efficiency in our inducible system (Figure 15B).

To prove whether the mutation in MH2 domain has an effect on TGF- $\beta$  signaling transduction, *SMAD4* KO and control organoids were treated with TGF- $\beta$ 1 and the expression of TGF- $\beta$  signaling target genes cell cycle growth arrest (*p21*, *GADD45B* and *AKAP12*) and epithelial-to-mesenchymal transition (*PAI-1*, *SMURF1*, *ITGB6*, *DLX2*) were analyzed by RT-PCR. While mRNA level of TGF- $\beta$  target genes were significantly upregulated in treated-control, the level in *SMAD4* KO cells were not different compare to untreated cell (Figure 15C and D). These findings confirmed the loss of *SMAD4*-TGF- $\beta$  signaling in iPSC-derived cholangiocyte organoids.

A



B

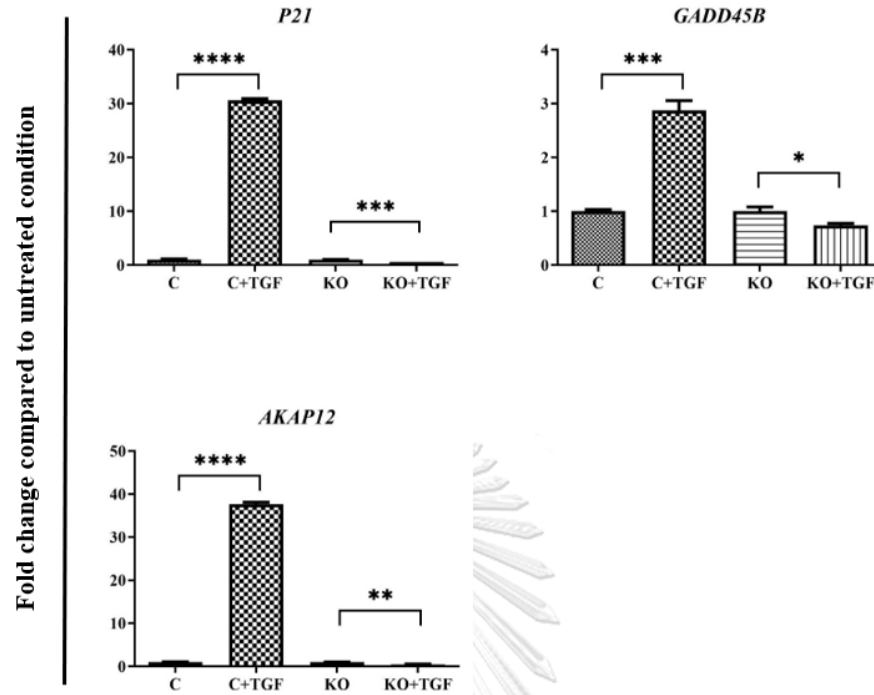


**Wildtype** 5'-GGAGGAGATCGCTTTTGTGGGTCAACTCTCCAATGCCACAGGACAGAAGCCATT-3'

**KO** GGAGGAGATCGCTTTTGTGGGTCAACTCT-----CCATT 21 bp del

**KO** GGAGGAGATCGCTTTTGTGGGTCAACTCTCAATGTT-----GACAGAAGCCATT 5 bp del

C



D

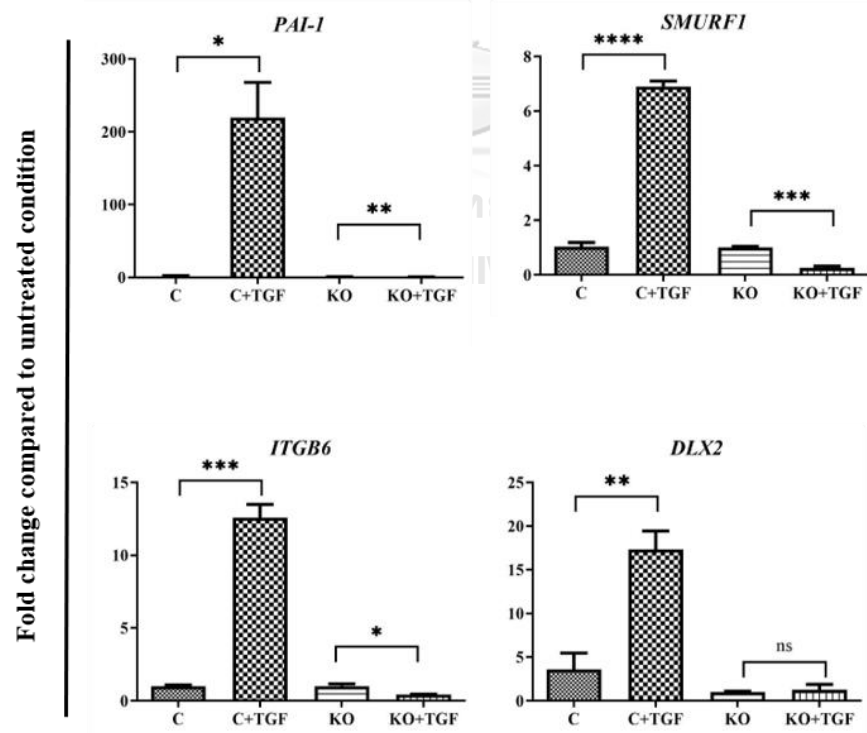


**Figure 15** Validation and TGF- $\beta$  transduction of *SMAD4* KO iPSC-derived cholangiocyte organoids. (A) Brightfield morphology of wildtype and *SMAD4* KO cholangiocyte organoids in selection medium with TGF- $\beta$ 1 and T7 endonuclease I mismatch detection of *SMAD4* gene knockout in *SMAD4* KO iPSC-derived cholangiocyte organoids. (B) Representative sequence patterns of *SMAD4* KO clone. (C) qRT-PCR analysis of TGF- $\beta$ /SMAD4 downstream target genes which are involved cytotostasis and (D) genes involved cell migration. Statistical analysis was analyzed by Student's t test, \* $P < 0.05$ , \*\* $P < 0.01$ , \*\*\* $P < 0.001$ , or nonsignificant (ns)  $P \geq 0.05$ . n = 3 biological replicates for each sample. C, *SMAD4* Wildtype iPSC-derived cholangiocyte organoids; KO, *SMAD4* KO-iPSC-derived cholangiocyte organoids; TGF, Transforming growth factor beta; *P21*, cyclin-dependent kinase inhibitor p21 ; *GADD45B*, Growth arrest and DNA-damage-inducible, beta; *AKAP12*, A-Kinase Anchoring Protein 12 ; *PAI-1*, Plasminogen activator inhibitor-1; *SMURF1*, E3 ubiquitin-protein ligase SMURF1; *ITGB6*, Integrin beta-6 ; *DLX2*, Distal-Less Homeobox 2.

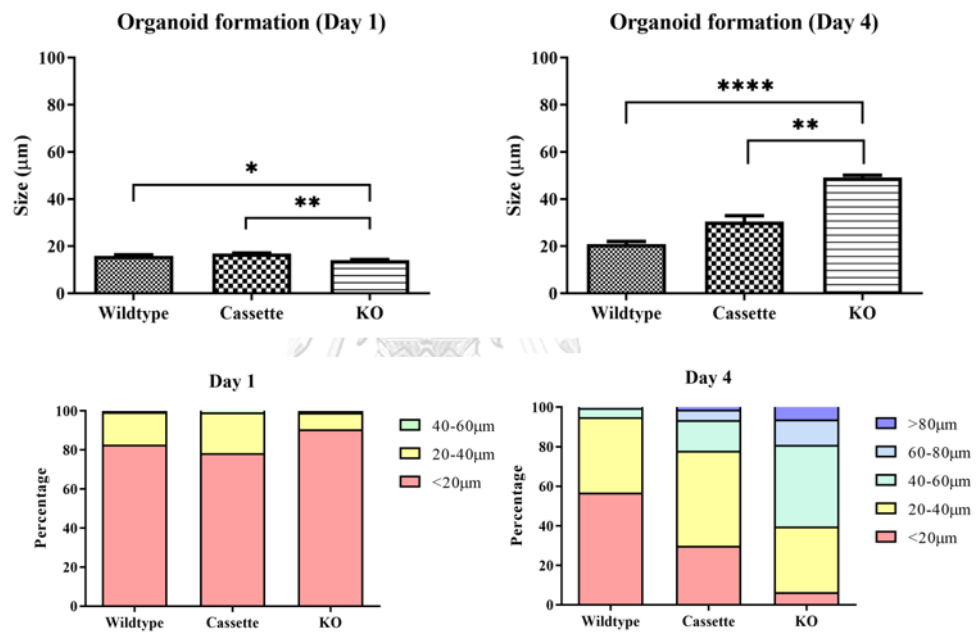
Previous study of Hernandez in 2019 reported the loss of SMAD4 promote cell proliferation in squamous cell carcinoma. While overexpression of SMAD4 in pancreatic cancer cell line promote TGF- $\beta$  Signaling dependent  $G_1$  arrest. (67)

So, we next investigate whether loss of SMAD4 function induce cell proliferation in iPSC-derived cholangiocyte organoid. Based on organoid formation assay, 24 hours after initiating culture the average organoid size in control-cassette and *SMAD4*-KO group were not significantly different, however at 96 hours the average *SMAD4*-KO organoid size were increased to  $49.2 \pm 1.56\% \mu\text{m}$  (mean  $\pm$  SD) whereas the average control-cassette size were increased in  $30.4 \mu\text{m} \pm 6.60\% \mu\text{m}$  (Figure 16A and B). Additionally, the organoid formation rate of *SMAD4*-KO line revealed higher number of organoids forming cell compared to control-cassette (39.7% vs 51.4%, control-cassette vs *SMAD4*-KO) (Figure 16C). Comprehensive transcriptome analysis demonstrated the differential gene expressions between control and *SMAD4*-KO lines (Figure 16D and E). Gene Ontology enrichment analysis indicated that upregulated differentially expressed genes (DEGs) in *SMAD4* KO iPSC-derived cholangiocyte organoids were particularly associated cell proliferation (MAPK, PI3K and Hippo signaling pathway) correspond to proliferation rate result, whereas the downregulated DEG was associated with cellular senescence (Figure 16F).

A

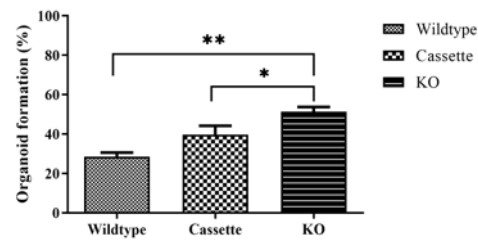


B



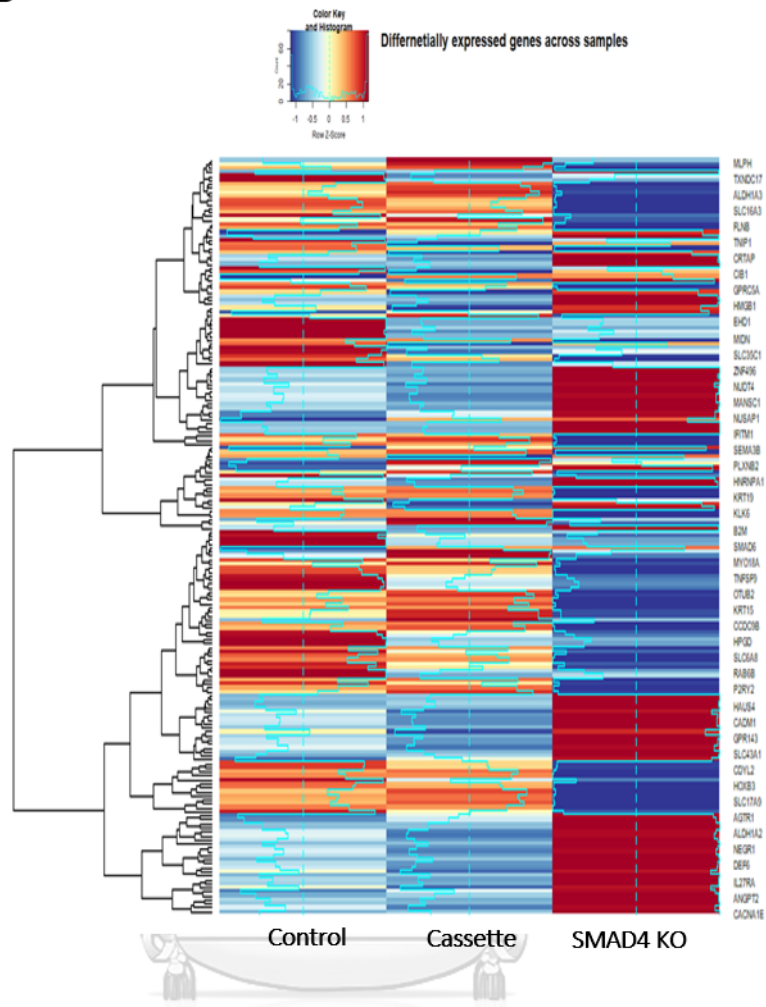
CHULALONGKORN UNIVERSITY

C



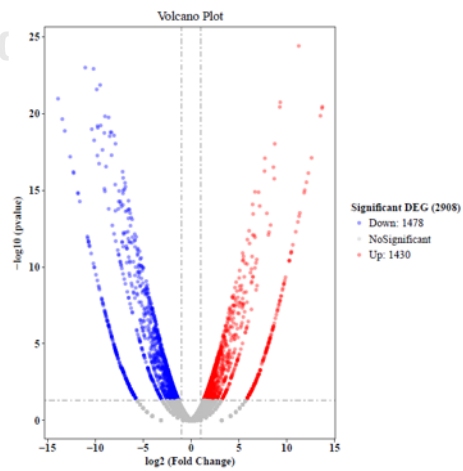


D



จุฬาลงกรณ์มหาวิทยาลัย  
CHULALONGKORN UNIVERSITY

E



F

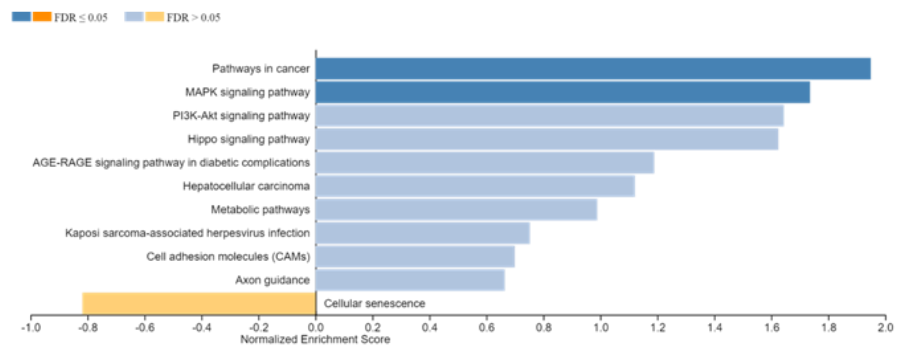


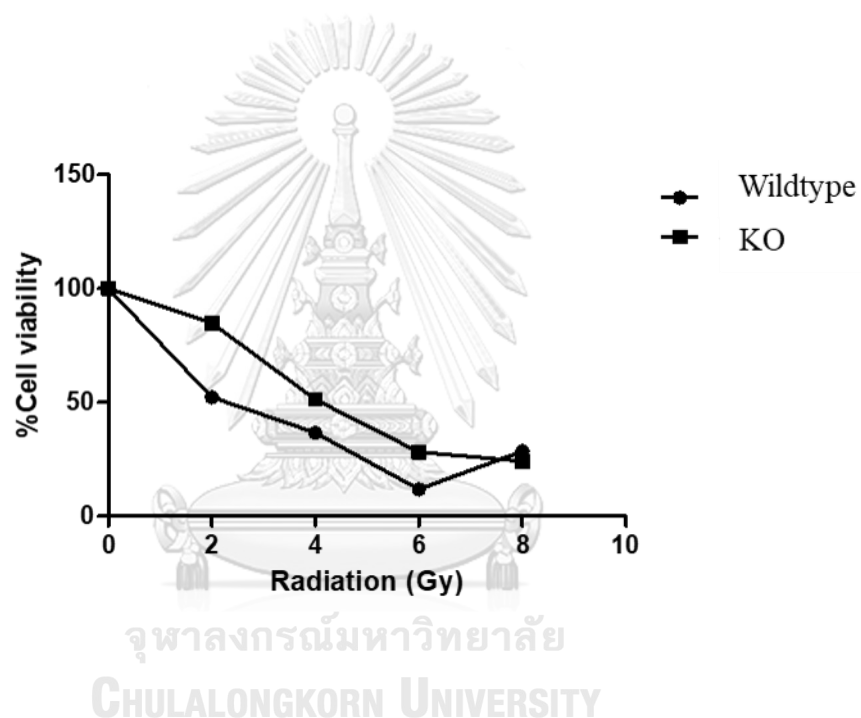
**Figure 16** Proliferation rate of *SMAD4* KO iPSC-derived cholangiocyte organoids.

(A) Brightfield images of organoid formation at 96 hours (B) Average organoid size (upper panel) and the representative proportion of organoid size (lower panel) at 24 hours and 96 hours. (C) Organoid formation efficiency. (D) Differentially expressed genes of control, cassette and *SMAD4* KO iPSC-derived cholangiocyte organoids. (E) Volcano plots of differential expressed genes between control and *SMAD4* KO iPSC-derived cholangiocyte organoids. (F) Gene ontology term enrichment of up-regulated and down-regulated genes in *SMAD4* KO iPSC-derived cholangiocyte organoids compare to control. Statistical analysis was analyzed by Student's t test, \* $P < 0.05$ , \*\* $P < 0.01$ , \*\*\* $P < 0.001$ , or nonsignificant (ns)  $P \geq 0.05$ .  $n = 3$  biological replicates for each sample. Control or Wildtype, *SMAD4* wildtype iPSC-derived cholangiocyte organoids; Cassette, Inducible *SMAD4* KO-PSC derived cholangiocyte organoids; KO, *SMAD4* KO-iPSC-derived cholangiocyte organoids.

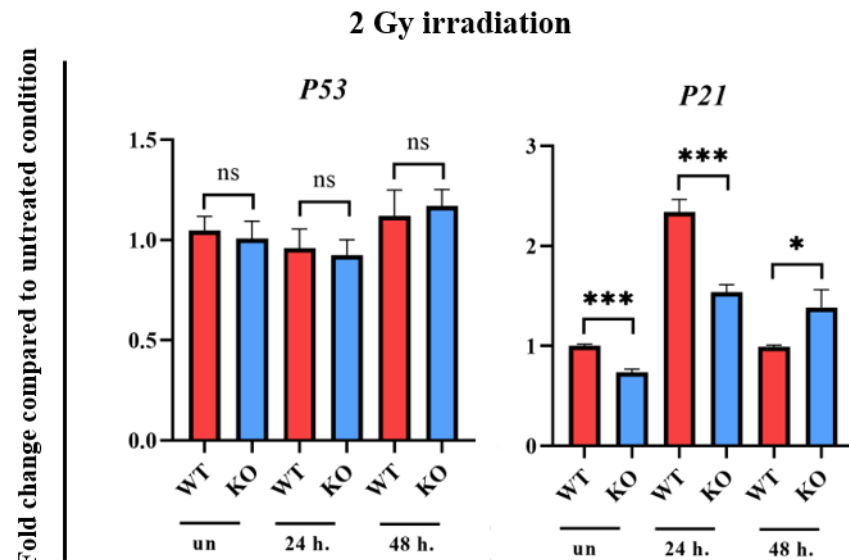
Next, we test the effect of *SMAD4* loss on DNA damage-induced stress. iPSC-derived cholangiocyte organoids were exposed gamma-radiation at vary dose and cell viability were measured 4 days after radiation. The finding revealed that survival rate of *SMAD4* KO iPSC-derived cholangiocyte organoids was higher than the control. Interestingly, at 2 Gy the survival rate of *SMAD4*-KO iPSC-derived cholangiocyte organoids was 84% whereas the survival of control organoid was reduced to 54% (Figure 17A). Increasing of radiation concentration, the different of survival rate was decreased and no effect at 8 Gy. Then, the expression of *p53* and *p21* of irradiated cells at 2 Gy and 6 Gy radiation were analyzed by RT-PCR. At 2 Gy, the expression of *p53* in control cell and *SMAD4*-KO cells at 24 hours was not increased, whereas the 2.34-fold upregulation of *p21* were observed in control but still slightly increased to

1.53-fold in *SMAD4*-KO iPSC-derived cholangiocyte organoids (Figure 17B). This finding was associated with the cell death that observed in at 2 Gy radiation. At 6 Gy, high radiation concentration induced the upregulation of *p53* both in control and *SMAD4*-KO cells. The upregulation of *p21* in 6 Gy radiation was significantly upregulated to 5-fold in control and 3.8-fold in *SMAD4*-KO iPSC-derived cholangiocyte organoids (Figure 17C). Our finding demonstrated that after radiation in absence of *SMAD4*, *p21* activation after injury was reduced, which enhance the cell survival rate, especially in lower concentration.

A



B



C

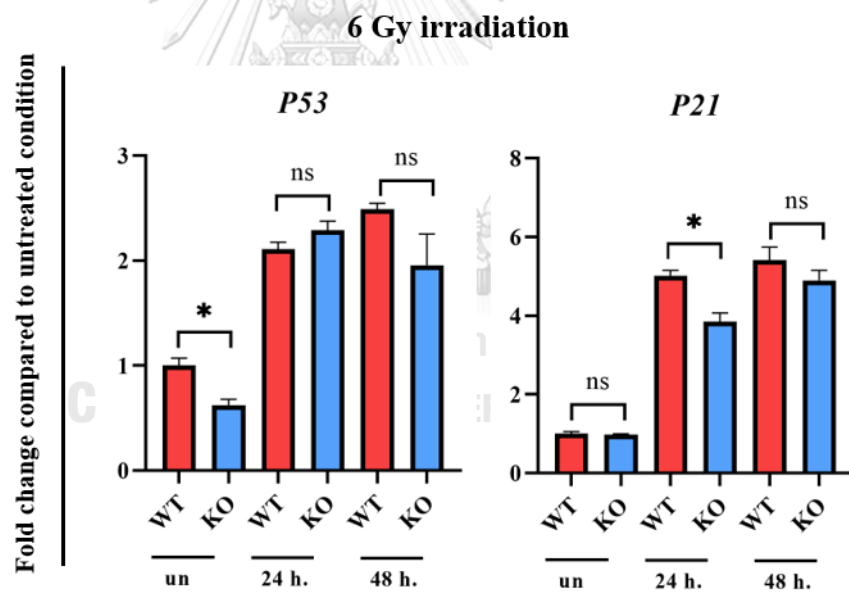


**Figure 17** Cell viability and the expression of *p53* and *p21* in *SMAD4* KO iPSC-derived cholangiocyte organoids after irradiation.

(A) Cell viability after irradiation at 96 hours. (B) qRT-PCR analysis of *p53* and *p21* expression level with 2 Gy of irradiation and (C) 6 Gy irradiation. Statistical analysis was analyzed by Student's t test, \* $P < 0.05$ , \*\*\* $P < 0.001$ , or nonsignificant (ns)  $P \geq 0.05$ .  $n = 3$  biological replicates for each sample. Wildtype, *SMAD4* wildtype iPSC-derived cholangiocyte organoids; Cassette, Inducible

*SMAD4* KO-PSC derived cholangiocyte organoids; KO, *SMAD4* KO-iPSC-derived cholangiocyte organoids.

TGF- $\beta$ /SMAD4 signaling pathway is crucial for cholangiocyte differentiation and tubular morphogenesis. We next examine whether loss of SMAD4 affect the tubular morphogenesis of iPSC-derived cholangiocyte organoid. As expected, duct-like structure was not detected in *SMAD4*-KO iPSC-derived cholangiocyte organoids throughout the differentiation day (Figure 18A). *SMAD4*-KO line retained its cyst structure whereas tubular formation was clearly observed since day 2 of differentiation in control. This result indicated the defect in tubular morphogenesis of *SMAD4*-KO iPSC-derived cholangiocyte organoids

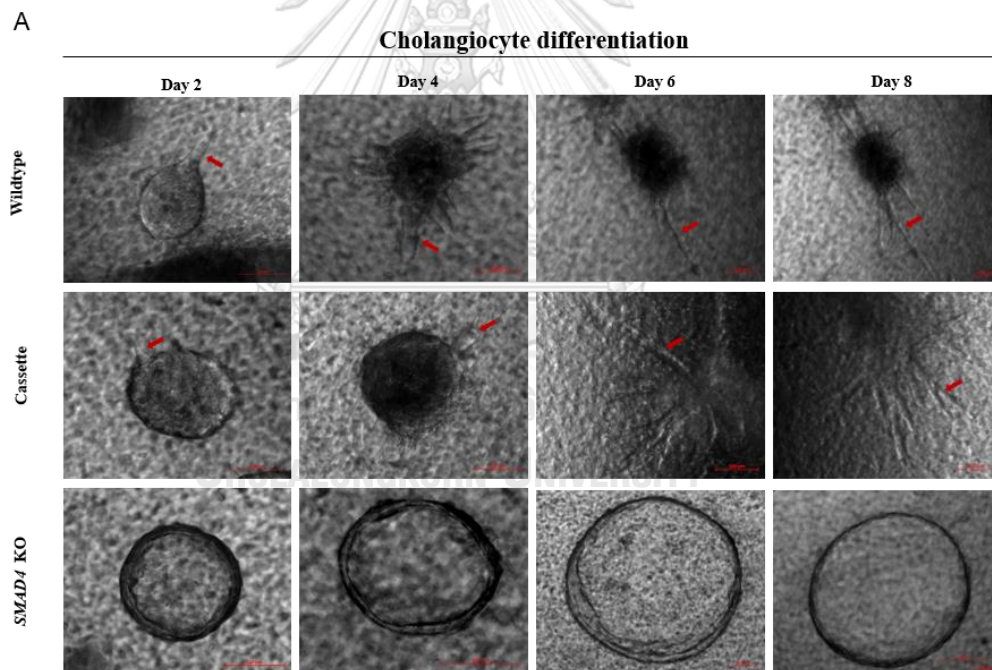


**Figure 18** Differentiation of mature cholangiocyte of *SMAD4* KO iPSC-derived cholangiocyte organoids.

(A) Light microscopy images of cholangiocyte differentiation. Red arrow indicate duct-like formation. Wildtype, *SMAD4* wildtype iPSC-derived cholangiocyte organoids; Cassette, Inducible *SMAD4* KO-PSC derived cholangiocyte organoids; KO, *SMAD4* KO-iPSC-derived cholangiocyte organoids.



จุฬาลงกรณ์มหาวิทยาลัย  
**CHULALONGKORN UNIVERSITY**

## CHAPTER V

### DISCUSSION

The limitation of primary cholangiocyte culture and expansion are obstacle of biliary pathology study for drug testing. (68) Currently, functional human cholangiocyte protocols from induced pluripotent stem cells (iPSCs) have been reported in several studies for using as alternative disease modeling to bridge the gap. (20, 22, 23) Due to the long-time of differentiation process and small number of cholangiocyte production, the combination of required growth factors in adult liver organoid culture medium in previous reports were used in this study. (60, 69) Our iPSC-derived cholangiocyte organoids, cholangiocyte progenitor, revealed the proliferating potential to long-term culture (more than 8 months) and containing cholangiocyte-associated gene expression profiles. Thus, our findings can effectively provide the alternative tool to generate large number of human cholangiocytes for many applications. Interestingly, we demonstrated that iPSC-derived cholangiocyte organoid cultured in this condition has potential to differentiate into hepatocyte-like cells with hepatocyte-specific gene expression profile. Our finding was correlated with recent reports which showing cell plasticity of liver during injury events. (70) In further study, it is still required more testing in order to validate whether these hepatocyte-like-cell has genuinely hepatocyte function as human hepatocytes and whether it can be used for disease modeling and cell therapy.

Compare to adult liver organoid culture, iPSC-based model provides the opportunity to study the roles of genes that critical for early developmental stage of hepatobiliary tract. Moreover, effective protocols using CRISPR/Cas9 technique to downregulate target genes in several adult organoids have been developed. (58, 65, 71, 72) it is still difficult to disrupt gene and transfection in mature cells, primary cholangiocytes. Our results demonstrated the using inducible CRISPR/ Cas9-engineered iPSCs model, we can promote gene knockout in human cells in any

developmental stage including more differentiated stage, cholangiocyte-like-cells, in the same way as conditional knockout animal models. In our system, during cholangiocyte differentiation in iPSC revealed low gene disruption rate as a result of the silenced Tet-On promoter during differentiation. We will further optimize the promoter selection and culture condition to improving the mutation rate effectiveness in iPSC-based model.

To generate resembling human cell model, we ask whether the expression of fetal genes remain exhibited in our iPSC-based model. We observed the expression of *LIN28B* in iPSC-derived cholangiocyte organoid, whereas it was not found in adult liver organoids. To the extent of our knowledge, *LIN28B* is RNA-binding protein which play role as a regulator in cell proliferation, differentiation, and metabolism. (73) iPSC-derived cholangiocyte organoid will be further investigate the function of this gene. It should be underlined that *LIN28B* reactivation has been reported in late stage of cancer as well as hepatocellular carcinoma. It also promotes the cancer aggressiveness. (74) Our system may provide useful model for *LIN28B*-expressed cells study.

Compare to progenitor cell which obtained from adult tissues, Currently, there was a few studies of iPSC-derived cholangiocyte progenitor. The BMP/TGF $\beta$ /SMAD signaling are known to play important roles in fate decision during liver and bile ducts development including repair process and cell-type-specific gene expression. BMP/TGF $\beta$ /SMAD signaling aberration can promote or inhibit carcinogenesis in a cell-specific and context-dependent manner. (75) *SMAD4* mutation in extrahepatic cholangiocarcinoma has been reported approximately 5-10%. (76, 77) However, the *SMAD4* mutation rate is significant higher in both intrahepatic and extrahepatic CCA with *O. viverrini*-associated CCA in Thailand (16.1-23.9%). (78, 79) Interestingly, the detection of *SMAD4* mutation was found in primary sclerosing cholangitis-derived tissue. (80) It has been unclear whether how *SMAD4* loss contribute to cholangiocarcinogenesis. In this study, we used our inducible CRISPR/Cas9 iPSC system for investigate the role of *SMAD4* in human cholangiocyte progenitors. Our results showed that *SMAD4* knockout iPSC-derived cholangiocyte



progenitors exhibited higher proliferation rate and colony-forming capacity compared to wildtype. Additionally, it also revealed elevating resistant to radiation.

According to co-regulator, SMAD4 are required for activating the expression of *P53* downstream target which involved in DNA damage response (P21). (81, 82) The study of whole transcriptomics would provide more data for understanding the role of *SMAD4* in these cells. Taken together, our finding revealed the accelerating carcinogenesis. It is still unclear whether *SMAD4* aberration alone in cholangiocyte progenitors would be sufficient for cancer initiation in this study. It has been reported that *SMAD4* mutation can initiate tumor formation and progression in head-and-neck squamous cell carcinoma. (83) Loss of *SMAD4* alone is insufficient to induce the pancreatic cancer formation but can promote cancer metastasis. (84) In animal model, *SMAD4* knockout in hepatocytes and bile duct epithelial cells alone revealed insufficient to induce CCA. However, CCA was developed high rate when combining with *PTEN*. (55) The investigation of cancer initiation potential in *SMAD4* KO cholangiocyte organoid or mature cholangiocyte will be observed in NSG mice. Additionally, it would be test whether chronic carcinogen exposure in vitro could induce these cells into CCA in vivo.

To summarize, we generate and validate a new effective system for investigate gene function in normal human liver and biliary cells. In this study, we demonstrate that *SMAD4* loss is sufficient to promote cholangiocyte progenitor proliferation, clonal expansion as well as protect from radiation injury-induced cell death. Therefore, these cells revealed the enhancement of tumor formation potential. Due to controllable of SgRNA in this system, it can be change or combine with any SgRNA to disrupt genes of interest in specific cell type. This system will be a potential tool in liver research as well as investigate cell origin of CCA in future study.

## REFERENCES

1. Chan-On W, Nairismagi ML, Ong CK, Lim WK, Dima S, Pairojkul C, et al. Exome sequencing identifies distinct mutational patterns in liver fluke-related and non-infection-related bile duct cancers. *Nature genetics*. 2013;45(12):1474-8.
2. Zhao M, Mishra L, Deng C-X. The role of TGF- $\beta$ /SMAD4 signaling in cancer. *Int J Biol Sci*. 2018;14(2):111-23.
3. Li W, Li L, Hui L. Cell Plasticity in Liver Regeneration. *Trends in Cell Biology*. 2020;30(4):329-38.
4. Kozaka K, Sasaki M, Fujii T, Harada K, Zen Y, Sato Y, et al. A subgroup of intrahepatic cholangiocarcinoma with an infiltrating replacement growth pattern and a resemblance to reactive proliferating bile ductules: 'bile ductular carcinoma'. *Histopathology*. 2007;51(3):390-400.
5. Nakanuma Y, Sato Y, Harada K, Sasaki M, Xu J, Ikeda H. Pathological classification of intrahepatic cholangiocarcinoma based on a new concept. *World J Hepatol*. 2010;2(12):419-27.
6. Liu C, Wang J, Ou Q-J. Possible stem cell origin of human cholangiocarcinoma. *World J Gastroenterol*. 2004;10(22):3374-6.
7. Cardinale V, Carpino G, Reid L, Gaudio E, Alvaro D. Multiple cells of origin in cholangiocarcinoma underlie biological, epidemiological and clinical heterogeneity. *World J Gastrointest Oncol*. 2012;4(5):94-102.
8. Banales JM, Huebert RC, Karlsen T, Strazzabosco M, LaRusso NF, Gores GJ. Cholangiocyte pathobiology. *Nature Reviews Gastroenterology & Hepatology*. 2019;16(5):269-81.
9. Tabibian JH, Masyuk AI, Masyuk TV, O'Hara SP, LaRusso NF. Physiology of cholangiocytes. *Compr Physiol*. 2013;3(1):541-65.
10. Han Y, Glaser S, Meng F, Francis H, Marzioni M, McDaniel K, et al. Recent advances in the morphological and functional heterogeneity of the biliary epithelium. *Experimental biology and medicine (Maywood, NJ)*. 2013;238(5):549-65.

11. Gordillo M, Evans T, Gouon-Evans V. Orchestrating liver development. *Development*. 2015;142(12):2094-108.
12. Si-Tayeb K, Lemaigre FP, Duncan SA. Organogenesis and Development of the Liver. *Developmental Cell*. 2010;18(2):175-89.
13. Huppert S, Campbell K. Bile Duct Development and the Notch Signaling Pathway: Pathogenesis and Clinical Management. 2018. p. 11-31.
14. Du C, Feng Y, Qiu D, Xu Y, Pang M, Cai N, et al. Highly efficient and expedited hepatic differentiation from human pluripotent stem cells by pure small-molecule cocktails. *Stem Cell Res Ther*. 2018;9(1):58-.
15. Gieseck RL, 3rd, Hannan NR, Bort R, Hanley NA, Drake RA, Cameron GW, et al. Maturation of induced pluripotent stem cell derived hepatocytes by 3D-culture. *PloS one*. 2014;9(1):e86372.
16. Graffmann N, Ncube A, Wruck W, Adjaye J. Cell fate decisions of human iPSC-derived bipotential hepatoblasts depend on cell density. *PloS one*. 2018;13(7):e0200416-e.
17. Hannan NRF, Segeritz C-P, Touboul T, Vallier L. Production of hepatocyte-like cells from human pluripotent stem cells. *Nat Protoc*. 2013;8(2):430-7.
18. Rashidi H, Luu N-T, Alwahsh SM, Ginai M, Alhaque S, Dong H, et al. 3D human liver tissue from pluripotent stem cells displays stable phenotype in vitro and supports compromised liver function in vivo. *Arch Toxicol*. 2018;92(10):3117-29.
19. Tolosa L, Caron J, Hannoun Z, Antoni M, López S, Burks D, et al. Transplantation of hESC-derived hepatocytes protects mice from liver injury. *Stem Cell Res Ther*. 2015;6:246-.
20. Dianat N, Dubois-Pot-Schneider H, Steichen C, Desterke C, Leclerc P, Raveux A, et al. Generation of functional cholangiocyte-like cells from human pluripotent stem cells and HepaRG cells. *Hepatology*. 2014;60(2):700-14.
21. Sampaziotis F, Cardoso de Brito M, Madrigal P, Bertero A, Saeb-Parsy K, Soares FAC, et al. Cholangiocytes derived from human induced pluripotent stem cells for disease modeling and drug validation. *Nature Biotechnology*. 2015;33(8):845-52.

22. Sampaziotis F, de Brito MC, Geti I, Bertero A, Hannan NR, Vallier L. Directed differentiation of human induced pluripotent stem cells into functional cholangiocyte-like cells. *Nat Protoc.* 2017;12(4):814-27.
23. Ogawa M, Ogawa S, Bear CE, Ahmadi S, Chin S, Li B, et al. Directed differentiation of cholangiocytes from human pluripotent stem cells. *Nat Biotechnol.* 2015;33(8):853-61.
24. Carpino G, Morini S, Carotti S, Gaudio E. Hepatic Progenitor Cells and Biliary Tree Stem Cells. In: Radu-Ionita F, Pysopoulos NT, Jinga M, Tintoiu IC, Sun Z, Bontas E, editors. *Liver Diseases: A Multidisciplinary Textbook.* Cham: Springer International Publishing; 2020. p. 29-35.
25. Aizarani N, Saviano A, Sagar, Maily L, Durand S, Herman JS, et al. A human liver cell atlas reveals heterogeneity and epithelial progenitors. *Nature.* 2019;572(7768):199-204.
26. MacParland SA, Liu JC, Ma XZ, Innes BT, Bartczak AM, Gage BK, et al. Single cell RNA sequencing of human liver reveals distinct intrahepatic macrophage populations. *Nature communications.* 2018;9(1):4383.
27. Bridgewater J, Galle PR, Khan SA, Llovet JM, Park J-W, Patel T, et al. Guidelines for the diagnosis and management of intrahepatic cholangiocarcinoma. *Journal of Hepatology.* 2014;60(6):1268-89.
28. Blehacz B. Cholangiocarcinoma: Current Knowledge and New Developments. *Gut Liver.* 2017;11(1):13-26.
29. Prueksapanich P, Piyachaturawat P, Aumpansub P, Ridditid W, Chaiteerakij R, Rerknimitr R. Liver Fluke-Associated Biliary Tract Cancer. *Gut Liver.* 2018;12(3):236-45.
30. Maemura K, Natsugoe S, Takao S. Molecular mechanism of cholangiocarcinoma carcinogenesis. *Journal of Hepato-Biliary-Pancreatic Sciences.* 2014;21(10):754-60.
31. Pauklin S, Vallier L. Activin/Nodal signalling in stem cells. *Development.* 2015;142(4):607.
32. Neuzillet C, Tijeras-Raballand A, Cohen R, Cros J, Faivre S, Raymond E, et al. Targeting the TGF $\beta$  pathway for cancer therapy. *Pharmacology & Therapeutics.* 2015;147:22-31.

33. Fabregat I, Moreno-Càceres J, Sánchez A, Dooley S, Dewidar B, Giannelli G, et al. TGF- $\beta$  signalling and liver disease. *The FEBS journal*. 2016;283(12):2219-32.
34. Clotman F, Jacquemin P, Plumb-Rudewiez N, Pierreux CE, Van der Smissen P, Dietz HC, et al. Control of liver cell fate decision by a gradient of TGF beta signaling modulated by Onecut transcription factors. *Genes & development*. 2005;19(16):1849-54.
35. Mu X, Lin S, Yang J, Chen C, Chen Y, Herzig MC, et al. TGF- $\beta$  Signaling Is Often Attenuated during Hepatotumorigenesis, but Is Retained for the Malignancy of Hepatocellular Carcinoma Cells. *PLoS one*. 2013;8(5):e63436.
36. Shibata T, Arai Y, Totoki Y. Molecular genomic landscapes of hepatobiliary cancer. *Cancer Science*. 2018;109(5):1282-91.
37. Newell P, Villanueva A, Friedman SL, Koike K, Llovet JM. Experimental models of hepatocellular carcinoma. *Journal of hepatology*. 2008;48(5):858-79.
38. Lin Z-Y, Liang Z-X, Zhuang P-L, Chen J-W, Cao Y, Yan L-X, et al. Intrahepatic cholangiocarcinoma prognostic determination using pre-operative serum C-reactive protein levels. *BMC Cancer*. 2016;16(1):792.
39. Braicu C, Burz C, Berindan-Neagoe I, Balacescu O, Tantau M, Cristea V, et al. Molecular Markers in the Pathogenesis of Cholangiocarcinoma: Potential for Early Detection and Selection of Appropriate Treatment. *Gastroenterology Res*. 2009;2(3):132-40.
40. Vaquero J, Guedj N, Clapéron A, Nguyen Ho-Bouidoires TH, Paradis V, Fouassier L. Epithelial-mesenchymal transition in cholangiocarcinoma: From clinical evidence to regulatory networks. *Journal of Hepatology*. 2017;66(2):424-41.
41. Kang YK, Kim WH, Jang JJ. Expression of G1-S modulators (p53, p16, p27, cyclin D1, Rb) and Smad4/Dpc4 in intrahepatic cholangiocarcinoma. *Human Pathology*. 2002;33(9):877-83.
42. Marks EI, Yee NS. Molecular genetics and targeted therapeutics in biliary tract carcinoma. *World J Gastroenterol*. 2016;22(4):1335-47.
43. Hill M, Alexander W, Hezel A. Models of intrahepatic cholangiocarcinoma: novel tools and therapeutic applications. *Gastrointestinal Cancer: Targets and Therapy*.

2018;Volume 8:1-11.

44. Papageorgis P, Cheng K, Ozturk S, Gong Y, Lambert AW, Abdolmaleky HM, et al. Smad4 Inactivation Promotes Malignancy and Drug Resistance of Colon Cancer. *Cancer Research*. 2011;71(3):998.
45. Zhang B, Zhang B, Chen X, Bae S, Singh K, Washington MK, et al. Loss of Smad4 in colorectal cancer induces resistance to 5-fluorouracil through activating Akt pathway. *Br J Cancer*. 2014;110(4):946-57.
46. Kim B-G, Li C, Qiao W, Mamura M, Kasperczak B, Anver M, et al. Smad4 signalling in T cells is required for suppression of gastrointestinal cancer. *Nature*. 2006;441(7096):1015-9.
47. Means AL, Freeman TJ, Zhu J, Woodbury LG, Marincola-Smith P, Wu C, et al. Epithelial Smad4 Deletion Up-Regulates Inflammation and Promotes Inflammation-Associated Cancer. *Cellular and Molecular Gastroenterology and Hepatology*. 2018;6(3):257-76.
48. Furukawa T, Sunamura M, Horii A. Molecular mechanisms of pancreatic carcinogenesis. *Cancer Sci*. 2006;97(1):1-7.
49. Ahmed S, Bradshaw A-D, Gera S, Dewan MZ, Xu R. The TGF- $\beta$ /Smad4 Signaling Pathway in Pancreatic Carcinogenesis and Its Clinical Significance. *J Clin Med*. 2017;6(1):5.
50. Huang W, Navarro-Serer B, Jeong YJ, Chianchiano P, Xia L, Luchini C, et al. Pattern of invasion in human pancreatic cancer organoids is associated with loss of SMAD4 and clinical outcome. *Cancer Research*. 2020:canres.1523.2019.
51. Maruyama M, Kobayashi N, Westerman KA, Sakaguchi M, Allain JE, Totsugawa T, et al. Establishment of a highly differentiated immortalized human cholangiocyte cell line with SV40T and hTERT. *Transplantation*. 2004;77(3):446-51.
52. Kim DG, Park SY, You KR, Lee GB, Kim H, Moon WS, et al. Establishment and characterization of chromosomal aberrations in human cholangiocarcinoma cell lines by cross-species color banding. *Genes, chromosomes & cancer*. 2001;30(1):48-56.
53. Ku JL, Yoon KA, Kim IJ, Kim WH, Jang JY, Suh KS, et al. Establishment and

- characterisation of six human biliary tract cancer cell lines. *Br J Cancer*. 2002;87(2):187-93.
54. Vaeteewoottacharn K, Pairojkul C, Kariya R, Muisuk K, Imtawil K, Chamgramol Y, et al. Establishment of Highly Transplantable Cholangiocarcinoma Cell Lines from a Patient-Derived Xenograft Mouse Model. *Cells*. 2019;8(5):496.
55. Xu X, Kobayashi S, Qiao W, Li C, Xiao C, Radaeva S, et al. Induction of intrahepatic cholangiocellular carcinoma by liver-specific disruption of Smad4 and Pten in mice. *The Journal of clinical investigation*. 2006;116(7):1843-52.
56. O'Dell MR, Huang JL, Whitney-Miller CL, Deshpande V, Rothberg P, Grose V, et al. Kras(G12D) and p53 mutation cause primary intrahepatic cholangiocarcinoma. *Cancer Res*. 2012;72(6):1557-67.
57. Farazi PA, Zeisberg M, Glickman J, Zhang Y, Kalluri R, DePinho RA. Chronic bile duct injury associated with fibrotic matrix microenvironment provokes cholangiocarcinoma in p53-deficient mice. *Cancer Res*. 2006;66(13):6622-7.
58. Artegiani B, van Voorthuijsen L, Lindeboom RGH, Seinstra D, Heo I, Tapia P, et al. Probing the Tumor Suppressor Function of BAP1 in CRISPR-Engineered Human Liver Organoids. *Cell Stem Cell*. 2019;24(6):927-43.e6.
59. Lau HCH, Kranenburg O, Xiao H, Yu J. Organoid models of gastrointestinal cancers in basic and translational research. *Nature Reviews Gastroenterology & Hepatology*. 2020;17(4):203-22.
60. Huch M, Gehart H, van Boxtel R, Hamer K, Blokzijl F, Verstegen MM, et al. Long-term culture of genome-stable bipotent stem cells from adult human liver. *Cell*. 2015;160(1-2):299-312.
61. Murry CE, Keller G. Differentiation of Embryonic Stem Cells to Clinically Relevant Populations: Lessons from Embryonic Development. *Cell*. 2008;132(4):661-80.
62. Kim YK, Refaeli I, Brooks CR, Jing P, Gulieva RE, Hughes MR, et al. Gene-Edited Human Kidney Organoids Reveal Mechanisms of Disease in Podocyte Development. *Stem Cells*. 2017;35(12):2366-78.
63. Schwank G, Koo B-K, Sasselli V, Dekkers Johanna F, Heo I, Demircan T, et al.

Functional Repair of CFTR by CRISPR/Cas9 in Intestinal Stem Cell Organoids of Cystic Fibrosis Patients. *Cell Stem Cell*. 2013;13(6):653-8.

64. Bonner A. CRISPR/Cas9 Gene Editing and its Potential to Treat Common Diseases. *Biomedical Journal of Scientific & Technical Research*. 2018;5.

65. Matano M, Date S, Shimokawa M, Takano A, Fujii M, Ohta Y, et al. Modeling colorectal cancer using CRISPR-Cas9-mediated engineering of human intestinal organoids. *Nat Med*. 2015;21(3):256-62.

66. González F, Zhu Z, Shi ZD, Lelli K, Verma N, Li QV, et al. An iCRISPR platform for rapid, multiplexable, and inducible genome editing in human pluripotent stem cells. *Cell Stem Cell*. 2014;15(2):215-26.

67. Fullerton PT, Jr., Creighton CJ, Matzuk MM. Insights Into SMAD4 Loss in Pancreatic Cancer From Inducible Restoration of TGF- $\beta$  Signaling. *Mol Endocrinol*. 2015;29(10):1440-53.

68. Ghanekar A, Kamath BM. Cholangiocytes derived from induced pluripotent stem cells for disease modeling. *Current opinion in gastroenterology*. 2016;32(3):210-5.

69. Hu H, Gehart H, Artegiani B, López-Iglesias C, Dekkers F, Basak O, et al. Long-Term Expansion of Functional Mouse and Human Hepatocytes as 3D Organoids. *Cell*. 2018;175(6):1591-606.e19.

70. Raven A, Lu W-Y, Man TY, Ferreira-Gonzalez S, O'Duibhir E, Dwyer BJ, et al. Cholangiocytes act as facultative liver stem cells during impaired hepatocyte regeneration. *Nature*. 2017;547(7663):350-4.

71. Drost J, van Jaarsveld RH, Ponsioen B, Zimmerlin C, van Boxtel R, Buijs A, et al. Sequential cancer mutations in cultured human intestinal stem cells. *Nature*. 2015;521(7550):43-7.

72. Hendriks D, Clevers H, Artegiani B. CRISPR-Cas Tools and Their Application in Genetic Engineering of Human Stem Cells and Organoids. *Cell Stem Cell*. 2020;27(5):705-31.

73. Shyh-Chang N, Daley GQ. Lin28: primal regulator of growth and metabolism in stem cells. *Cell Stem Cell*. 2013;12(4):395-406.



74. Balzeau J, Menezes MR, Cao S, Hagan JP. The LIN28/let-7 Pathway in Cancer. *Frontiers in genetics*. 2017;8:31.
75. Ritterhouse LL, Wu EY, Kim WG, Dillon DA, Hirsch MS, Sholl LM, et al. Loss of SMAD4 protein expression in gastrointestinal and extra-gastrointestinal carcinomas. *Histopathology*. 2019;75(4):546-51.
76. Ito T, Sakurai-Yageta M, Goto A, Pairojkul C, Yongvanit P, Murakami Y. Genomic and transcriptional alterations of cholangiocarcinoma. *J Hepatobiliary Pancreat Sci*. 2014;21(6):380-7.
77. Tian W, Hu W, Shi X, Liu P, Ma X, Zhao W, et al. Comprehensive genomic profile of cholangiocarcinomas in China. *Oncology letters*. 2020;19(4):3101-10.
78. Ong CK, Subimerb C, Pairojkul C, Wongkham S, Cutcutache I, Yu W, et al. Exome sequencing of liver fluke-associated cholangiocarcinoma. *Nature genetics*. 2012;44(6):690-3.
79. Jusakul A, Kongpetch S, Teh BT. Genetics of *Opisthorchis viverrini*-related cholangiocarcinoma. *Current opinion in gastroenterology*. 2015;31(3):258-63.
80. Goeppert B, Folseraas T, Roessler S, Kloor M, Volckmar A-L, Endris V, et al. Genomic Characterization of Cholangiocarcinoma in Primary Sclerosing Cholangitis Reveals Therapeutic Opportunities. *Hepatology*. 2020;72(4):1253-66.
81. Atfi A, Baron R. p53 Brings a New Twist to the Smad Signaling Network. *Science Signaling*. 2008;1(26):pe33.
82. Pardali K, Kurisaki A, Morén A, ten Dijke P, Kardassis D, Moustakas A. Role of Smad proteins and transcription factor Sp1 in p21(Waf1/Cip1) regulation by transforming growth factor-beta. *The Journal of biological chemistry*. 2000;275(38):29244-56.
83. Bornstein S, White R, Malkoski S, Oka M, Han G, Cleaver T, et al. Smad4 loss in mice causes spontaneous head and neck cancer with increased genomic instability and inflammation. *The Journal of clinical investigation*. 2009;119(11):3408-19.
84. Malkoski SP, Wang XJ. Two sides of the story? Smad4 loss in pancreatic cancer versus head-and-neck cancer. *FEBS letters*. 2012;586(14):1984-92.



จุฬาลงกรณ์มหาวิทยาลัย  
**CHULALONGKORN UNIVERSITY**



จุฬาลงกรณ์มหาวิทยาลัย  
**CHULALONGKORN UNIVERSITY**

## VITA

**NAME** Natthida Kittimawikrom

**DATE OF BIRTH** 31 July 1994

**PLACE OF BIRTH** Bangkok

**INSTITUTIONS ATTENDED** 2012-2015 B.Sc. in Microbiology, Faculty of sciences, King Mongkut's University of Technology Thonburi

**HOME ADDRESS** 153/494, 89/1 Pracha Uthit Rd., Thung Khru, Thung Khru, Bangkok 10140, Thailand.

**PUBLICATION** Poster presentation  
Kittimawikrom N., Ingrungruanglert P., Israsena N. (May 1, 2020) "Establishment of Inducible SMAD4 Knockout PSC-Derived Cholangiocyte Committed Cells" poster presentation at The 5th RSU International Research Conference on Science and Technology, Social Sciences, and Humanities 2020, Rangsit University, Thailand